Dynamic Field of View Restriction in 360º Video: Aligning Optical Flow and Visual SLAM to Mitigate VIMS

PAULO BALA, FCT, Universidade Nova de Lisboa & ITI-LARSys, Portugal
IAN OAKLEY, Department of Human Factors Engineering, UNIST, South Korea
VALENTINA NISI, IST, Universidade de Lisboa & ITI-LARSys, Portugal
NUNO NUNES, IST, Universidade de Lisboa & ITI-LARSys, Portugal

Head-Mounted Display based Virtual Reality is proliferating. However, Visually Induced Motion Sickness (VIMS), which prevents many from using VR without discomfort, bars widespread adoption. Prior work has shown that limiting the Field of View (FoV) can reduce VIMS at a cost of also reducing presence. Systems that dynamically adjust a user's FoV may be able to balance these concerns. To explore this idea, we present a technique for standard 360º video that shrinks FoVs only during VIMS inducing scenes. It uses Visual Simultaneous Localization and Mapping and peripheral optical flow to compute camera movements and reduces FoV during rapid motion or optical flow. A user study (N=23) comparing 360º video with *unrestricted-FoVs* (90º), reduced *fixed-FoVs* (40º) and *dynamic-FoVs* (40º-90º) revealed that dynamic-FoVs mitigate VIMS while maintaining presence. We close by discussing the user experience of dynamic-FoVs and recommendations for how they can help make VR comfortable and immersive for all.

CCS Concepts: • **Human-centered computing → Virtual reality**; *Usability testing*.

Additional Key Words and Phrases: Visually Induced Motion Sickness; Cinematic Virtual Reality; Optical Flow; Simultaneous Localization and Mapping; Field of View Restriction;

ACM Reference Format:
Paulo Bala, Ian Oakley, Valentina Nisi, and Nuno Nunes. 2021. Dynamic Field of View Restriction in 360º Video: Aligning Optical Flow and Visual SLAM to Mitigate VIMS. In *CHI Conference on Human Factors in Computing Systems (CHI '21), May 8–13, 2021, Yokohama, Japan.* ACM, New York, NY, USA, 27 pages. https://doi.org/10.1145/3411764.3445499

1 INTRODUCTION

Virtual Reality (VR) has resurged as a medium for work and entertainment [3], bolstered by new consumer head-mounted displays (HMDs) [70], that are powerful enough to deliver engaging and immersive VR experiences and affordable enough to reach for mainstream adoption. While HMDs' advances in tracking, latency, refresh rate, resolution, and optics have substantially improved VR [2], key user experience issues still prevent many users from enjoying VR, and consequently, bar widespread adoption [29, 37, 94]. Among these barriers, Visually Induced Motion Sickness (VIMS), also commonly referred to as VR Sickness, is particularly prominent, as up to 67% of adults experience mild to severe symptoms such as nausea, dizziness, sweating and vomiting [94] and women are more likely to manifest symptoms than men [3, 46, 76].

The complex nature of VIMS has lead to a large body of literature [29, 98], exploring issues such as the polysymptomatic (multiple symptoms) and polygenic (different manifestation of symptoms) profile of users [51, 94], the difficulties in quantifying symptoms [4, 56, 59, 101], the impact of different technologies (e.g. CAVE, HMDs) [29, 98] and types of content (e.g. games, video) [29], proposing diverse theoretical accounts of the biological mechanisms of its symptoms [98] and exploring inconsistencies in the terminology used to describe it [51, 98]. A large number of prevention/reduction techniques for VIMS have been proposed and are mostly focused on HMD-based VR, and specifically for live computer generated environments [29, 98]. While some of these techniques have been shown to be effective, through manipulations such as restriction of a user's field of view (FoV) during rapid motion [41], they are currently incompatible with pre-rendered media formats such as 360º video.

This incompatibility matters because, while 360º video has been characterized as less immersive than computer generated VR [103], its realism, ease of use and affordability mean it is in widespread commercial use. It has also been deployed to achieve objectives such as prototyping [43] or to develop production-quality immersive content [12, 13]. Furthermore, research has explored how to augment 360º videos to make them influence and/or respond to behaviour [7, 52, 65, 66, 80, 86, 102]. Based on the prevalence and potential of the 360º video format, and the lack of existing VIMS mitigation techniques that can be applied to it, this paper explores how an existing popular VIMS mitigation strategy, FoV Restriction [17, 41], can be applied to 360º video. In addition, while this strategy has been shown to be successful in reducing VIMS by blocking peripheral motion stimulation during locomotion, it comes at the cost of lowering presence. Designed with the goal to be as unobtrusive as possible [41], systems that dynamically adjust the FoV [2, 8, 53, 63, 120] may be able to balance the trade-off between reducing VIMS and restricting presence.

Therefore, this paper presents a novel technique for Dynamic FoV Restriction in 360º videos. Firstly, we use Visual Simultaneous Localization and Mapping (SLAM) system [107] to differentiate between when the camera is static and when the camera is moving, and use this to apply VIMS mitigation only when there is movement. Secondly, we use the optical flow (motion pattern caused by the relative motion of objects compared to the camera/observer) of the user's peripheral vision, where optical flow is primarily detected [113], to determine the aperture of the FoV, restricting it in relation to the magnitude of peripheral optical flow. We evaluate our technique with a within-subjects user study (N=23) where we compare our technique (*dynamic-FoV*, ranging from 40º-90º) against two baselines: *unrestricted-FoV* (90º), where no FoV restriction is applied, and *fixed-FoV* (40º), where a fixed FoV restriction is applied throughout the video. Our findings show that *dynamic-FoV* is effective in reducing VIMS (to the levels achieved by *fixed-FoV*) and also maintains higher levels of presence (similar to those reported in *unrestricted-FoV*). *Dynamic-FoV* was found to be well received by most participants, and sometimes viewed as being part of the narrative of the video. The key contribution of this paper is the description of a novel technique for Dynamic FoV Restriction in 360º Video, validated by its empirical evaluation. Considering the need for design guidelines for VR and 360º video [7, 54, 68, 97], we conclude by discussing the user experience of dynamic-FoVs through the combination of data from questionnaires, run-time performance and semi-structured interviews, and delineate practical recommendations for including dynamic-FoVs in future experiences.

2 RELATED WORK

2.1 VIMS

The complex nature of VIMS has led to terms such as simulator sickness, cybersickness, and VR sickness [51, 98] to be used interchangeably when referring to the occurrence of motion sickness symptoms without real physical movement [51]. These symptoms are categorized as nausea (stomach awareness, sweating, salivation, etc.), oculomotor (headaches, eye strain, etc.) and disorientation (vertigo, dizziness, etc.) [56]. For VIMS, disorientation is the main symptom category [93] but oculomotor symptoms are also commonly reported [58], and symptoms are more severe when using HMDs compared to screen-based simulators [41]. Furthermore, multiple factors such as age [10], gender [76], exposure length [37], habituation [37], and type of content [50], have been identified as influencing the symptom profile and severity, complicating VIMS research with users. Several theories have emerged to explain VIMS [38, 95, 110], but the Cue Conflict or Sensory Mismatch theory remains the most widely accepted [58]. This theory posits that VIMS results from a mismatch between (or within) the visual, vestibular, and somatosensory senses [58, 62]. For this reason, VIMS mitigation strategies are concerned with reducing or eliminating sensory conflicts. In order to avoid these solutions disrupting VR experiences, researchers typically aim to design techniques that are imperceptible to users.

2.2 VIMS Mitigation

Many VIMS mitigation strategies focus on reducing the mismatch between visual and vestibular systems through hardware improvement, leading to high-precision low-latency tracking, high–frame-rate rendering, and short-persistence displays [41, 73, 117]. Other hardware augmentations involve either creating a real vestibular response to movement (e.g. through the use of omnidirectional rigs [31]), substituting proprioceptive feedback (e.g. use of smartphones' inertial sensors for "walking-in-place" [109], mapping pedaling in a mini exercise bike to walking in VR [45]) or inducing a fake vestibular response (e.g., using 2-sided step-synchronized vibrations motors behind the ears [88]). The use of internal/external tracking systems in consumer VR devices enables positional tracking, and subsequently, natural walking as locomotion in virtual environments [120]. When possible, this is preferred since it generates sensory signals (vestibular and proprioceptive) that match the visual virtual space [120]. When the tracking space is limited, redirected walking [92] is a possible solution, since the virtual environment is dynamically and imperceptibly rotated to keep users in the tracking space. When physical movement is not possible, when it does not match its virtual counterpart (e.g. walking vs. flying), or when there is limited tracking space, artificial locomotion techniques through the use of remote controllers are preferred [25]. These controllers can be used for teleportation through target selection [14], moving the user to the selected viewpoint instantly, avoiding sensory conflict from virtual movement, but leading to spatial disorientation and reduced presence. Controllers can also be used for joystick/steering-based movement, but again generate discrepancies between visual and vestibular systems [3]. When traveling long distances in areas with visual similarities, Freitag et al. [44] used dynamic speed in steering, "skipping" those areas without increasing discomfort. Additionally, several works [24, 27, 41] have used the speed of movement from a controller as input for their VIMS mitigation strategies.

The previously mentioned strategies are primarily focused on walking-based or non-natural travel techniques [78] for computer-generated environments, where the user is able to move virtually. In 360º video, the user has no agency in translational movement as they are dependent on the camera's movement. Since these strategies are incompatible, VIMS Mitigation for 360º video is focused on visual optimization of the stimuli, rather than the user. Among the possible visual optimizations, rest-frames are elements present in the virtual environment that remain fixed in relation to the real world regardless of the user behaviour [90]. In particular, adding rest-frames that are fixed to the head reference frame, referred to as independent visual backgrounds, such as grids [35, 36, 82], clouds [64] or a virtual nose [114, 116], have been show to mitigate VIMS, although contrary studies exist [121]. Cao et al. [27] have also proven the efficacy of dynamic rest-frames in reducing VIMS, with the opacity of the added visual element being dynamically controlled by the virtual movement. Other visual optimizations of the stimuli include blurring non-salient objects [5, 83], blurring rotational movement [5, 23], head locking to avoid rotational movement [5, 55], simulated "blinking" during fast movement [5, 39], the "circle effect" [24, 71] (multi-camera, with a fixed peripheral ring and moving center) and the "dot effect" [5, 24] (moving peripheral orbs countering the virtual direction). The most popular visual optimization, and one that is often seen in studies involving 360° video, is FoV restriction, which we will review more extensively.

2.2.1 Field of View (FoV) Restriction. Peripheral vision (due to the existence of rods in the retina [111, 113]) is more sensitive to motion from optical flow [11, 21]. Restricting peripheral vision in the FoV is effective since it blocks the peripheral stimulation that causes sensory mismatches. When discussing FoV in HMDs, it is important to distinguish the display FoV (area of the visual field occupied by the display) from the camera FoV (area of the visual environment that is drawn in the display) [89]. The display FoV is a physical characteristic of the HMD, while the camera FoV is a software characteristic, therefore, runtime FoV restriction refers solely to camera FoV. There is conflicting evidence as to whether or not differences between the display and camera FoV cause discomfort [34, 75], but wide FoVs are generally considered to induce more VIMS symptoms compared to narrow FoVs [34]. However, FoV restriction can occur unintentionally due to the physical design of HMDs. While modern HMD development seeks to increase the display FoV (and subsequently the camera FoV) towards the limits of human binocular vision (up to 190°) [33, 118], current mid-tier consumer VR headsets more commonly feature a FoV of approximately 110° [77]. For some users, real FoVs may be reduced by variations in facial structures, padding on HMDs and hidden area masks (areas that are not rendered). In these ways, HMDs can restrict peripheral vision without intervention. However, since future HMDs will try to match human binocular vision (up to 190°), it is expected the prevalence and severity of VIMS symptoms to increase in the future.

FoV Restriction through software, also known as "vignetting" or "tunneling" [1, 85], is one of most popular VIMS mitigation strategies, and is recommended by major companies in the area, such as Oculus [85] and Google [1], used in popular applications such as Google Earth VR [48] and incorporated into games as an optional "Comfort Mode" [84]. Fixed FoVs restriction has been shown to reduce VIMS [19, 57, 100, 112]. However, it has also been linked to reduced task performance in visual searches [112] and a reduced sense of presence [100]. Dynamic FoVs, which are adjusted in size continuously, are a potential way to counteract these negative outcomes. They have been widely deployed. For example, using physiological sensors, Kim et al. [60] detected when participants were experiencing VIMS and restricted the FoV and notified users to stop and relax. Fernandes and Feiner [41] used input speed from a gamepad to determine the size of a FoV restriction, leading to reduced VIMS. This work has also inspired studies investigating sex-bias in FoV Restriction [3], dynamic-FoV based on self reported comfort [120], the technique's usage in a commercial HMD game [108], and the design of a dynamic foveated FoV for HMDs that incorporates gaze tracking [2]. Moreover, Norouzi et al. [84] investigated the use of dynamic FoV restriction in amplified head rotation, but found that the use of FoV restriction resulted in a statistically significant increase in symptoms.

FoV restriction strategies have also been applied to 360° video. Existing work has focused on replacing input from a gamepad, as seen in Fernandes and Feiner [41], with input from the video itself, generated through computer vision algorithms. When "scrubbing" through footage in their VR editor, Nguyen et al. [81] use the shakiness of the 360° video (measured through a Lucas-Kanade algorithm for optical flow) to determine the FoV size. Kala et al. [53] used feature extraction and a Lucas-Kanade algorithm for optical flow in a 360° video of a roller coaster to determine the size of the vertical FoV in an attempt to simulate blinking. In an extension to this work, Lim et al. [63] use a predicted sickness score (calculated through the content analysis of the video similar to Kala et al. [53] and head dispersion of the user) to dynamically adjust the FoV. Both Kala et al. [53] and Lim et al. [63] do not use validated scores for sickness or presence, so the efficacy of these strategies in reducing VIMS is debatable. Finally, Bala et al. [8] used optical flow

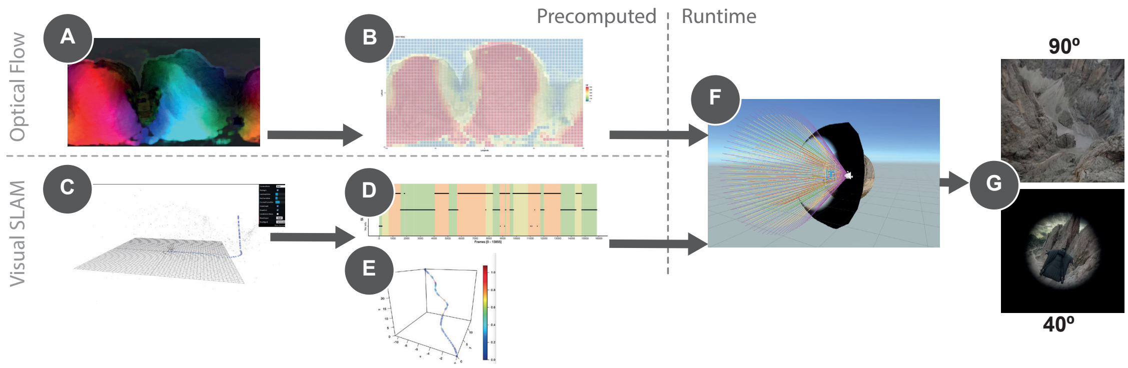

Fig. 1. Dynamic FoV Restriction pipeline: A) Optical Flow through Gunnar Farnebäck, B) Grid grouping of Optical Flow values (see supplementary files for video), C) OpenVSLAM's camera pose estimation, D) Automatic movement classification based on OpenVSLAM's tracking, E) Map and speed estimation based on OpenVSLAM's tracking, F) Optical Flow polling based on series of peripheral concentric rings, G) Dynamic FoV restriction between 40° and 90°.

(through a Gunnar Farnebäck algorithm) to control user's exposure to an independent visual background or/and to a FoV Restrictor in a short 360° video of a roller coaster. Although they did not report statistically reduced VIMS, they did note their strategies allowed for increased exploration when compared to a baseline. These works are tested in extreme case videos (e.g. roller coasters), therefore are not generalizable to existing commercial content and do not explore the impact of strategies on the overall user experience.

This prior work on applying optical flow and FoV restriction to 360° video has motivated us to explore further use of computer vision algorithms to mitigate VIMS, how to make these methods more generalizable to diverse video content and to understand their impact not only on VIMS reduction but as well as the user experience.

3 DESIGN OF DYNAMIC FOV RESTRICTION

In this section, we describe the design of our novel dynamic FoV restriction system for 360° video. We combine precomputed optical flow detection with an equirectangular Visual SLAM to detect moments of visual motion that may trigger or exacerbate VIMS, and seek to rectify or mollify these by adjusting the displayed FoV in real-time. To the best of our knowledge, ours is the first system to apply SLAM to 360° video for VIMS mitigation, as well as to use optical flow from peripheral vision. We present the details of our system design in the sections below.

3.1 Optical Flow

Optical flow is a motion pattern between consecutive frames caused by the relative movement of the environment and the camera. Sparse optical flow algorithms (e.g. Lucas-Kanede [6], as used in Kala et al. [53]) return only a limited set of flow vectors based on identifiable features, while dense optical flow (e.g. Gunnar Farnebäck [40], as used in Bala et al. [8]) return flow vectors for all pixels. This latter algorithm is also more computationally expensive but since video processing can be pre-computed, we chose to use a dense optical flow as it is more accurate. Optical Flow was calculated in Python, using OpenCV 3 [20], a open-source library of computer vision algorithms (see A in Fig. 1). Firstly, considering the large format of video, we resampled the video to a width of 640 pixels for faster processing and to a constant bit rate. We extended the borders of the video by 5% of its width and height and copied the opposing image data to the borders, as done by Chou et al. [30]; this was done considering the visual discontinuity of borders in equirectangular images that produce optical flow artefacts in the edges of an image. For the optical flow, we used two pyramid layers, an image scale of 0.3, a single search iteration per pyramid level, a window size of 10, and a pixel neighborhood of 5. Before saving the optical flow magnitude, values from the added border padding were cropped. To reduce file size, optical flow was only saved every 5 frames, and values were grouped in 5x5 pixel squares to form a grid (see B in Fig. 1). Optical flow magnitude was saved in a comma-separated values (CSV) file.

3.2 Visual SLAM

Visual Odometry (VO) and Simultaneous Localization and Mapping (SLAM) systems are crucial components in robotics and mobile vision applications [28]. Visual Odometry is a process of estimating motion of an agent based on camera input, while in SLAM systems, an agent must localize itself and build a map of the environment, without any prior knowledge [119]. VO's focus is on local consistency, while SLAM systems are more concerned with the global consistency of the map (e.g. loop closures and reducing drift using external sensors) [119]. Visual SLAMs, whose main input source is video, use feature/keypoint extraction to compute geometrical information [119]. OpenVSLAM [107] is an open-source system using an indirect SLAM algorithm with sparse features and is compatible with monocular, stereo, and RGB-D cameras (see C in Fig. 1). To the best of our knowledge, OpenVSLAM is the first open-source Visual SLAM framework that can accept equirectangular videos. OpenVSLAM has 3 main modules: a tracking module (frame by frame estimation of camera pose and creation of keyframes), a mapping module (uses keyframes to triangulate landmarks and create/extend the map), and a global optimization module (loop detection and pose-graph optimization). To achieve compatibility with different cameras, OpenVSLAM relies on a configuration file specifying parameters of the camera/video and feature extraction (we used 3000 as a maximum number of keypoints, 1.3 scale factor, 12 levels, and a mask disabling feature extraction in the top and bottom 10% of height). OpenVSLAM is primarily used for single scene videos, so we extended the source code to be compatible with videos with several scenes. If tracking is lost (e.g. when scene changes or when there are not enough trackable features), the system tries relocalization for 3 seconds; if the system is not able to relocate, output files are exported, the system is reset and a new map is created. We extended the output files to not only save the map database in the default MessagePack format but to also save a CSV with the result of tracking (timestamp, frame number, tracking state, position and rotation of the camera, number of keypoints found/tracked, number of landmarks found/tracked). Based on this data, we were able to visualize the camera path in 3D space and calculate speed and acceleration (see E in Fig. 1) in R [91]. While these motion paths were consistent with the camera movement, we were not able to maintain a consistent measure of speed/acceleration between scenes to be able to use it as input. Future inclusion of sensor data from an inertial measurement unit might be able to resolve this issue. Joining the tracking data from different maps, SLAM tracking (see D in Fig. 1)was dichotomised as "movement", "stationary", and "no info" (e.g. when the mapping module is initializing and is not possible to determine movement). Short tracking outliers caused by relocalization were filtered out before saving SLAM tracking data to a CVS file.

3.3 Restricted FoV

Our VR prototype was made in Unity (release 2020.2) for the Oculus Go, using the "Tunneling Demo" [1] from Google Daydream Elements as a basis for the implementation of FoV restriction. Considering a $diameter_{inner}$ and $diameter_{outer}$ for the FoV, the tunneling effect can be separated into three parts: an inner space where the content is visible, a transition space where the content is partially visible, and outer space where the content is completely blocked. The transition space is equivalent to 10° and when we mention FoV size we are referring to $diameter_{inner}$. Considering the Oculus Go, an FoV size of 90° corresponds to the effect not being visible (see G in Fig. 1). Considering the limits of peripheral vision and the threshold for color perception at 60° [67], an FoV size of 40° (plus 20° of transition space) corresponds to the effect blocking mid-peripheral and far peripheral vision (see G in Fig. 1). This FoV size is consistent with previous work [3, 120].

For the Dynamic FoV, during runtime, SLAM tracking data is polled one second ahead of the current frame to determine if the camera is moving or stationary (taking a conservative approach, "no info" is treated as moving). If the camera is moving, optical flow values are polled one second ahead of the current frame. These values are polled using a series of concentric rings of different diameters (see F in Fig. 1) to represent the peripheral vision, as proposed by Lungaro et al. [67] for video streaming. Each ring represents a series of ray-casters (with the origin on the virtual camera) that identify squares in the optical flow grid. We used 5 rings, starting at a diameter of 50° (increase of 10° for each ring) with 50 ray-casters (increase of 10 rays for each ring) to model peripheral vision. To prevent ray-casters from different rings focusing on the same square, the rings are rotated around the axis of the camera (increase of 5° for each ring) and raycasted squares are filtered to be unique. During runtime, the absolute optical flow magnitude of unique raycasted squares is averaged. This polled magnitude is used to determine the size of FoV. We empirically found that the relation between polled magnitude and FoV size worked better with a polled magnitude of 50 corresponding to a minimum FoV of 40° and a min magnitude of 15 corresponding to a maximum FoV of 90°. Therefore, FoV size is calculated from linear interpolation of these values and smooth damped (gradually changing a value towards a desired goal over time) over one second. Polling ahead of time, averaging magnitude and smooth dampening were used to reduce interference from outliers (which might lead to infrequent flickering of FoV size).

4 USER STUDY

4.1 Media

Considering the goal of the study of evaluating the effectiveness of our design candidate, we carefully selected video source material with considerable motion and duration, multiple scenes, and scenes with multiple points of interest. Existing 360° Video data sets (e.g [32, 79]) mostly contain brief clips that are not sufficiently long to meet duration recommendations for VIMS studies [105]. Therefore, we chose a commercially produced video, "Tales from the Edge" [9], produced by GoPro and RYOT, where a wingsuit pilot flies through the Italian Alps to honor a fallen colleague. We trimmed the end credits of the video to yield a clip with a duration of 8'49" (from 9'15" originally). Apart from its rich narrative story, the video offers a variety of interesting scenes to test our algorithms (e.g. scene shot by drone, 3D generated scene, etc.). To provide baseline data about the video contents, in terms of scene cuts or changes in scene locomotion, two researchers individually divided the video into intervals and then merged their classifications into the contents shown in table 1. Intervals in this process were manually classified as "stationary" (in green), "slow" (in yellow, generally corresponding to rotational movement from the sway of a handheld or worn camera) and "fast" (in orange, corresponding to fast translational movement such as flying).

We applied our optical flow and SLAM algorithms to this video. Fig. 2 represents a time series of the video, with plots for optical flow magnitude, tracked landmarks by the Visual SLAM, and the automatic classification of movement from the SLAM tracking. The background colour of the plots represents the manual classification of intervals (table 1). Our automatic classification (bottom of fig 2) is generally consistent with the manual classification, being able to distinguish movement (yellow and orange) from stationary shots (green). Mismatches between manual and automatic classification are due to the re-localization interval used in the Visual SLAM algorithm. While this interval could be

Table 1. Manual classification of the level of motion in the video used in the study. We identify 28 intervals, each classified with one of three levels of motion. Green shows "stationary" intervals (217.95s), yellow shows "slow" motion (85.54s), orange shows "fast" motion (224.23s).

	Frames	Start Time	Duration	Description
I_1	1-210	0”	6.97s	RYOT and GoPro logo.
I_2	211-690	7”	15.97s	Two wingsuit pilots are preparing to jump the Dolomites, Italy. Camera is attached to helmet.
I_3	691-1543	23”	28.4s	The pilots jumped, with the lead pilot is ahead of the camera direction.
I_4	1544-1865	51”	10.7s	"Tales from the Edge" logo.
I_5	1866-2219	1’ 2”	11.77s	The two pilots walk across a field.
I_6	2220-2523	1’ 14”	10.1s	The two pilots are walking across a hill.
I_7	2524-4041	1’ 24”	50.57s	Static shot of a mountain, where a 2D video is projected onto a wall.
I_8	4042-5056	2’ 15”	33.8s	Drone footage of a climber, that quickly flys away from the climber.
I_9	5057-5327	2’ 49”	9s	Stationary shot of lead pilot sitting and talking.
I_{10}	5327-5653	2’ 58”	10.87s	Stationary shot of lead pilot getting into the wingsuit.
I_{11}	5654-7754	3’ 8”	70s	Two pilots jump at "The Fingers". Camera is attached to lead pilot.
I_{12}	7755-8272	4’ 18”	17.23s	Two pilots are talking in a field. Camera is handheld by the lead pilot.
I_{13}	8273-8588	4’ 36”	10.5s	Stationary shot of lead pilot sitting and talking.
I_{14}	8589-8772	4’ 46”	6.1s	Stationary shot of mountain.
I_{15}	8773-9155	4’ 52”	12.73s	3D computer generated mountain. Camera shows trajectory of jump and moves to specific points.
I_{16}	9156-9218	5’ 5”	2.07s	Stationary shot of mountain.
I_{17}	9219-9506	5’ 7”	9.57s	Stationary shot inside a moving cable car.
I_{18}	9507-9774	5’ 17”	8.9s	Stationary shot of ’Death Star’ mountain
I_{19}	9775-10119	5’ 26”	11.47s	Secondary pilot prepares for jump. Camera is attached to helmet.
I_{20}	10120-10858	5’ 37”	24.6s	Lead pilot prepares for jump. Camera is attached to body.
I_{21}	10859-11311	6’ 2”	15.07s	Lead pilot jumps.
I_{22}	11312-11748	6’ 17”	14.53s	Secondary pilot jumps.
I_{23}	11749-11998	6’ 32”	8.3s	Stationary shot in the mountain of pilots flying across.
I_{24}	11999-13203	6’ 40”	40.13s	Lead pilot exits the mountain and deploys parachute.
I_{25}	13204-14251	7’ 20”	34.9s	Stationary shot of field landing.
I_{26}	14252-14740	7’ 55”	16.27s	Two pilots are talking after the field landing. Camera is handheld by the lead pilot.
I_{27}	14741-14881	8’ 11”	4.67s	Stationary shot of lead pilot sitting and talking.
I_{28}	14882-15858	8’ 16”	32.53s	Stationary shot of pilots preparing to jump, while a 2D Video is projected onto a mountain wall

reduced, re-localization is important for cases where Visual SLAMs have difficulty in extracting features (e.g. fast rotation of camera or abnormally fast movement). The latter can be observed in I_{21} with abrupt drops of tracked landmarks. Optical flow magnitude values are also consistent with the intervals, with higher values in intervals with movements and peaks caused by scene transitions.

4.2 Experimental Design

This study used a repeated measures design, comparing our design candidate (*dynamic-FoV*) with two baselines (*unrestricted-FoV* and *Fixed-FoV*) in the viewing of the selected 360° video using an HMD. The *unrestricted-FoV* (u-FoV) condition corresponds to an FoV of 90° (the maximum FoV for the device used and where no effect is noticeable); the *Fixed-FoV* (f-FoV) condition corresponds to an FoV of 40° (the necessary amount to block near mid-peripheral and far-peripheral vision). The *dynamic-FoV* (d-FoV) condition corresponds to an FoV between 40° and 90° (calculated through the peripheral optical flow) only when there is movement (indicated through the automatic classification from the Visual SLAM). When stationary, *dynamic-FoV* condition presents an FoV of 90°, similarly to *unrestricted-FoV*. To prevent order effects, conditions were counterbalanced in a Latin squares design. To minimize after-exposure symptoms, sessions were scheduled with at least a day apart, and participants were free to reschedule if they felt symptoms prior

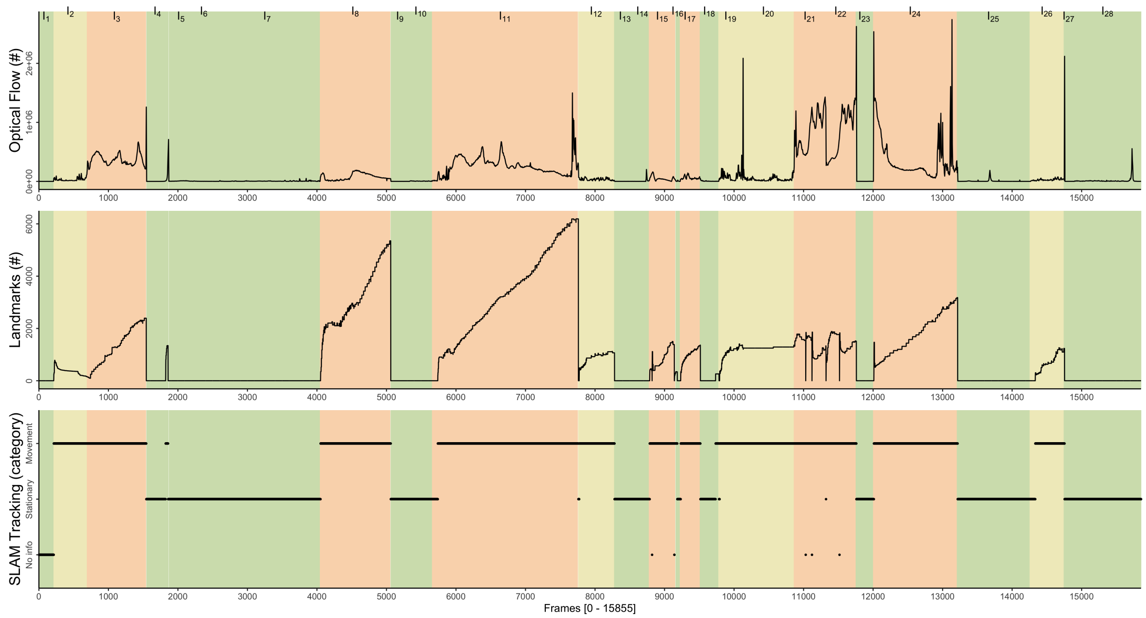

Fig. 2. Time series of optical flow (top), tracked landmarks in OpenVSLAM (center), and automatic movement classification based on OpenVSLAM’s tracking (bottom). Colors show the manual classifications of the motion in each time interval (green: stationary; yellow: slow; orange: fast)

to the session. Throughout the paper, we use the same color scheme for images and tables: *unrestricted-FoV* in red, *dynamic-FoV* in purple, and *Fixed-FoV* in blue.

4.3 Measures

Prior to the first session, participants were asked to fill a demographic questionnaire with gender, age, and items on experience with VR and 360º video (rating scale with seven levels, "Never" to "Very often"). Additionally, participants filled out the Motion Sickness Susceptibility Questionnaire Shortform (MSSQ-Short) [47].

Before and after each session, participants filled out a Pre-exposure and Post-exposure Simulator Sickness Questionnaire (SSQ), composed of 16 items rated in 4 levels ("None", "Slight", "Moderate" and "Severe"). The difference between Post and Pre values is used to calculate 4 components: Disorientation (SSQ-D), Nausea (SSQ-N), OculoMotor (SSQ-O) and Total Severity (SSQ-TS). Through the same items but with a different weight calculation, we also used the Virtual Reality Sickness Questionnaire (VRSQ), which Kim et al. [59] claim to be more appropriate for experiences in HMDs. The difference between Post and Pre values is used to calculate 3 items: Disorientation (VRSQ-D), OculoMotor (VRSQ-O), and Total Severity (VRSQ-TS).

During each session, head direction (quaternions) was captured periodically and saved on the device in a CVS file. During each session, head direction was polled on average 2641 times or approximately five times per second. Post-study, head direction data was retrieved and converted into Angles (angle between one recording to the next, in radians), Axes (Yaw, Pitch, Roll, in radians), and geographic coordinates (Longitude and Latitude, in degrees).

After each session, participants filled out the Igroup Presence Questionnaire (IPQ) [99], a validated *Presence* scale composed of 4 components: Spatial Presence (SP), Involvement (INV), Experienced Realism (ER) and General Presence (GP).

Following Fernandes et al. [41], we had participants fill out a Visual Questionnaire (VQ), aimed at determining the effects of visual optimizations on the participant's experiences. In its first section, participants are asked to identify if a set of given *Visual Statements* (VS) occurred using seven level Likert scales ("Did not notice or did not happen" to "Very obvious"). The following seven VSs were used: VS1 "I saw the virtual environment get smaller or larger"; VS2 "I saw the virtual environment flicker"; VS3 "I saw the virtual environment get brighter or dimmer"; VS4 "I saw that something in the virtual environment had changed color"; VS5 "I felt like my field of view was changing in size"; VS6 "I felt like I was getting bigger or smaller"; VS7 "I saw that something in the virtual environment had changed size". In the second and third sections, Most Noticed Visual Change (MNVC) and Second Most Noticed Visual Change (SMNVC), participants are asked to identify a particular noticed VS. If participants identify a VS, follow up Likert scales (all with seven levels) request them to self-report their confidence ("Not confident" to "Very confident") and to rate the VS in terms of Comfort ("Not comfortable" to "Very comfortable"), Enjoyability ("Less enjoyable" to "More enjoyable") and Desire ("Don't want" to "Definitely want").

After each session, in order to gather information on participant's perception of the 360° video and the effect on any visual optimization, we conducted a semi-structured interview asking about how the session went and any discomfort they might have felt, and, if participants mentioned the visual optimization, opening the scope of inquiry to question about their effect and/or why they happened.

4.4 Experimental Procedure & Setup

Convenience sampling was used for multiple reasons. Firstly, since the experience spanned multiple sessions, over a period of a week or more, participants needed to be easily accessible. Secondly, and most importantly, the COVID-19 epidemic made it unfeasible to recruit external participants. The study was carried out in a lab in a geographically isolated region with fewer than 100 total cases at the time, and in accordance with local laws. Following guidelines for HCI studies [106], lab personnel and infrastructure were used, and participants were not monetarily compensated for taking part in the study. Furthermore, as suggested by Steed et al. [106], a combination of hygienic measures (disinfectant wipes, disposable masks, ultraviolet light decontamination, etc.) was used between sessions.

Before the first session, participants were given an informed consent form with the overall goal of the study, but no information about possible visual optimizations. In the first session, participants were asked to fill a questionnaire with demographic data, and before viewing the 360° video, were asked to fill a Pre-Session questionnaire. Participants were able to adjust the HMD and were asked to stand up (so that changes in head movement data reflect postural sway) before the researcher started the experience with the HMD's remote controller. A meeting room in our research laboratory, clear of obstructive furniture, was used for all sessions. A mobile Oculus Go HMD was used and due to COVID-19 concerns, no headphones were used, relying on the HMD's audio output. After each session, participants were asked to fill a Post-Session questionnaire and to participate in a semi-structured interview.

4.5 Sample

Due to the influence of several factors in VIMS susceptibility (e.g. age, gender, previous experience, etc.) and the small available pool of participants due to COVID-19, we did not assume any inclusion or exclusion criteria for the population, other than being able to complete the viewing task. All participants (N = 23, 35% female) completed all sessions in their entirety. The mean age among participants was 28.3 years (SD = 6.6 years; range = 19-49).

Data analysis was done for the full population as well as for a subpopulation made of participants in the upper 75th percentile of the MMSQ-short (participants more susceptible to motion sickness). A separate analysis of subpopulations more prone to motion sickness can also be found in McGill et al. [71]. The mean age among participants in this subpopulation (N = 15, 33% female) was 29.33 years (SD = 7.6 years; range = 20-49). Additional subpopulations (e.g. only females) were not considered due to the small sample size (N<12).

4.6 Analysis

Analysis was conducted in R [91], using a 2-tailed testing at α of .05 and figures were produced using the ggplot2 package [115]. Testing for Assumption of Normality was done through visual analysis of histograms/boxplots/Q-Q plots, analysis of Kurtosis and Skewness (and their standard errors), and normality tests (Shapiro-Wilk, given that N<50). All data (except for presence components) was not normally distributed and thus failed to satisfy the assumptions required for parametric testing.

Angles (how much the head moves between readings) were accumulated according to the manual classification of intervals ("stationary", "slow", "fast") and automatic classification from Visual SLAM ("stationary" and "movement"). For these measures, outliers were removed [42] and the resulting missing data imputed via multivariate chained equations [26, 49]. The resulting data were found to be normally distributed.

Measures in which data were normal were analyzed with one-way repeated measures ANOVAs, while measures in which data failed normality checks were analyzed with Friedman tests. For ANOVAs, Greenhouse-Geisser corrected degrees of freedom are reported for cases where sphericity was violated [69]. Post-hoc testing was conducted with t-tests for parametric data and Friedman's Aligned Ranks tests for non-parametric data. All post-hoc pairwise comparisons include Holm-Bonferroni confidence interval adjustments. Unless explicitly stated, all statistical data reported, tables, and images correspond to the full participant population.

For plots involving map projections, the following packages were used: sf [87], rgdal [16], spdep [15], and mapproj [72]. For hotspot analysis, we used a Getis-Ord Gi* algorithm, using 2-tailed testing at α of .05, consistent with Rothe and Hußmann [96] and Bala et al. [7].

Interviews were recorded, transcribed, and then analyzed by two researchers using MaxQDA [61, 104]. Through an iterative process, we thematically analyzed [22] session transcripts, clustered for each condition, by sorting into categories according to the main topic of the statements. Finally, we clustered themes that were common in the different conditions and themes that were specific to a particular condition.

5 RESULTS

5.1 Sample

Concerning motion sickness susceptibility for our **full population**, our population is representative of a general population since the mean raw MSSQ score of 9.261 (SD = 8.29; range = 0-34) is below the population norm of (SD = 9.90) [47]. Likewise, the population is inexperienced with VR and 360° video. In terms of items related to previous experience, most participants (57% and 52%, respectively) reported very seldom experience with VR (mdn = 1, iqr = 1) and 360° video (mdn = 1, iqr = 0).

Table 2. Median scores and standard deviations for SSQ and VRSQ components across conditions *unrestricted-FoV*(u-FoV), *dynamic-FoV*(d-FoV), and *fixed-FoV*(f-FoV), considering the full population (top) and upper 75th percentile subpopulation (bottom). Total Severity (TS) scores are highlighted in light grey. Kendall's W effect size uses the Cohen's interpretation guidelines of small (0.1-0.3), moderate (0.3-0.5) and strong (>0.5).

			Unrestricted-FoV	*Dynamic-FoV*	*Fixed-FoV*	Main Effect	Effect Size	d-FoV vs u-FoV	d-FoV vs f-FoV	f-FoV vs u-FoV
Full	SSQ	TS	14.96 ± 15.37	0 ± 20.35	11.22 ± 10.44	$\chi^2(2) = 9.887$, p = 0.007	W = 0.215	p = 0.047	-	-
		D	13.92 ± 28.44	0 ± 32.49	0 ± 16.6	$\chi^2(2) = 8.13$, p = 0.017	W = 0.177	-	-	p = 0.018
		O	7.58 ± 13.05	0 ± 14.08	7.58 ± 10.59	-	-	-	-	
		N	9.54 ± 11.49	0 ± 16.83	0 ± 13.07	$\chi^2(2) = 8$, p = 0.018	W = 0.178	p = 0.046	-	-
	VRSQ	TS	7.50 ± 9.44	0 ± 9.31	0.83 ± 5.61	$\chi^2(2) = 11.34$, p = 0.003	W = 0.344	p = 0.04	-	p = 0.02
		D	6.67 ± 10.02	0 ± 8.67	0 ± 5.99	$\chi^2(2) = 15.83$, p < 0.001	W = 0.246	p = 0.012	-	p = 0.006
		O	8.33 ± 10.95	0 ± 10.61	0 ± 7.46	-	-	-	-	-
Upper 75th	SSQ	TS	18.7 ± 17	0 ± 24.32	11.22 ± 10.85	$\chi^2(2) = 10.12$, p = 0.05	W = 0.338	p = 0.049	-	-
		D	27.84 ± 31.04	0 ± 38.9	0 ± 18.87	$\chi^2(2) = 8.391$, p = 0.015	W = 0.280	-	-	p = 0.028
		O	7.58 ± 12.96	0 ± 15.55	7.58 ± 10.12	-	-	-	-	-
		N	9.54 ± 12.32	0 ± 20.23	0 ± 12.39	-	-	-	-	-
	VRSQ	TS	10.83 ± 9.91	0 ± 10.54	4.17 ± 5.76	$\chi^2(2) = 13.06$, p = 0.001	W = 0.435	-	-	p = 0.009
		D	13.33 ± 9.91	0 ± 10.04	0 ± 6.60	$\chi^2(2)=14.37$, p < 0.001	W = 0.479	p = 0.049	-	p = 0.006
		O	8.33 ± 10.82	0 ± 11.87	8.33 ± 6.90	-	-	-	-	-

Table 3. Mean scores and standard error for IPQ components across conditions, considering the full population (top) and upper 75th subpopulation percentile (bottom)

			Unrestricted-FoV	*Dynamic-FoV*	*Fixed-FoV*
Full	IPQ	GP	3.78 ± 0.27	3.65 ± 0.30	3.09 ± 0.30
		SP	4.14 ± 0.17	3.70 ± 0.23	3.33 ± 0.25
		INV	3.11 ± 0.13	3.19 ± 0.16	2.92 ± 0.17
		ER	2.73 ± 0.13	2.57 ± 0.16	2.51 ± 0.09
Upper 75th	IPQ	GP	3.8 ± 0.34	3.53 ± 0.34	2.93 ± 0.38
		SP	4.2 ± 0.25	3.57 ± 0.25	3.12 ± 0.33
		INV	3.13 ± 0.16	3.2 ± 0.21	2.75 ± 0.20
		ER	2.62 ± 0.17	2.38 ± 0.21	2.45 ± 0.13

5.2 Self-Reported Measures

5.2.1 SSQ & VRSQ. Table 2 includes the median and standard deviation scores for SSQ and VRSQ components, for the full population and upper 75th percentile subpopulation. All post-hoc pairwise comparisons used a Holm-Bonferroni correction.

5.2.2 Presence. Table 3 includes the mean and standard error for presence components, for the full population and upper 75th percentile subpopulation. Considering the **full population**:

- For GP, Mauchly's test indicated that the assumption of sphericity had been violated, $\chi^2(2) = 0.7514$, p = 0.05, therefore degrees of freedom were corrected using Greenhouse-Geisser estimates of sphericity ($\epsilon = 0.8$). The results show statistically significant differences for GP, F(1.6, 35.24) = 4.105, p = 0.023, $\eta^2 = 0.05$. Post-hoc paired comparisons with Holm-Bonferroni correction indicate a significantly higher value for *unrestricted-FoV* compared to *fixed-FoV* (p = 0.044).
- For SP, Mauchly's test indicated that the assumption of sphericity had been violated, $\chi^2(2) = 0.643$, p = 0.01, therefore degrees of freedom were corrected using Greenhouse-Geisser estimates of sphericity ($\epsilon = 0.737$). The results show statistically significant differences for SP, F(1.47, 32.42) = 6.723, p = 0.003, $\eta^2 = 0.09$. Post-hoc

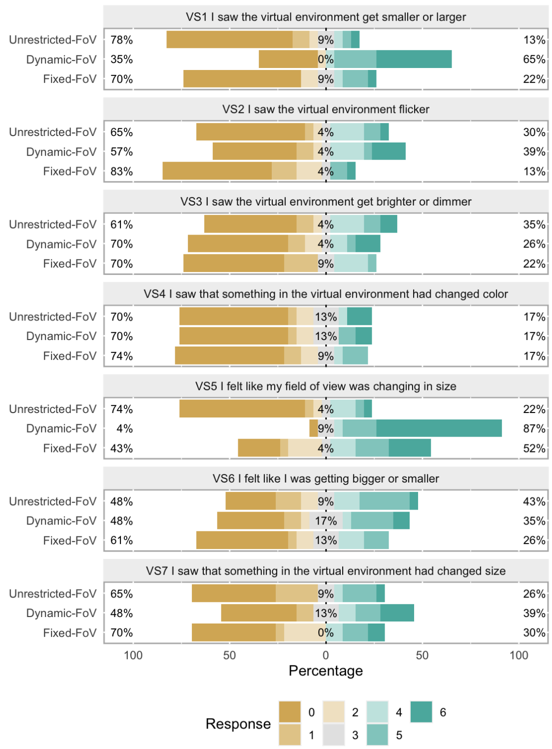

Fig. 3. Stacked barplot for Visual Questionnaire (VS1 to VS7), where response 0 is equal to "Did not notice or did not happen" and 6 to "Very obvious"

paired comparisons with Holm-Bonferroni correction indicate a significantly higher values for *unrestricted-FoV* compared to *fixed-FoV* (p = 0.008) and for *unrestricted-FoV* compared to *dynamic-FoV* (p = 0.011).

Considering the **upper 75th percentile subpopulation**:

- For SP, Mauchly’s test indicated that the assumption of sphericity had been violated, $\chi^2(2) = 0.291$, $p < 0.001$, therefore degrees of freedom were corrected using Greenhouse-Geisser estimates of sphericity ($\epsilon = 0.585$). The results show statistically significant differences for SP, F(1.17, 16.38) = 7.944, p = 0.002, $\eta^2 = 0.153$. Post-hoc paired comparisons with Holm-Bonferroni correction indicate significantly higher values for *unrestricted-FoV* compared to *fixed-FoV* (p = 0.012) and for *unrestricted-FoV* compared to *dynamic-FoV* (p = 0.000168).

5.2.3 Visual Questionnaire. Figure 3 shows the stacked barplots for VS1 to VS7, and participants are in agreement as to whether they happened across conditions, except for VS1 and VS5:

- For VS1, there was a statistically significant difference, $\chi^2(2) = 11.1$, $p < 0.001$. Post-hoc pairwise comparisons using Holm-Bonferroni correction show significantly higher values for *dynamic-FoV* compared to *unrestricted-FoV* (p = 0.005) and for *dynamic-FoV* compared to *fixed-FoV* (p = 0.009).

- For VS5, there was a statistically significant difference, $\chi^2(2) = 24.03$, $p < 0.001$. Post-hoc pairwise comparisons using Holm-Bonferroni correction indicated significantly higher values for *dynamic-FoV* compared to *unrestricted-FoV* (p = 0.000259), for *dynamic-FoV* compared to *fixed-FoV* (p = 0.002) and for *fixed-FoV* compared to *unrestricted-FoV* (p = 0.008).

5.2.4 MNVC & SMNVC. Based on the previous significance, we look only at VS5 ("I felt like my field of view was changing in size") in *dynamic-FoV* and *fixed-FoV* and VS1 ("I saw the virtual environment get smaller or larger") for *dynamic-FoV*.

In *dynamic-FoV*, most participants (15, out of 21) chose VS5 as the MNVC, and 11 of them with a high degree of confidence (mdn = 6, iqr = 0.5). For these 15 participants, most reported both comfort (mdn = 3; iqr = 2) and enjoyability (mdn = 3, iqr = 2.5) around the center of the scale, but responses for future desire was more diverse (mdn = 2, iqr = 3). For VS1, only 2 participants chose it with a high degree of confidence (mdn = 6, iqr = 0) and reported values for comfort, enjoyability and desire (4,5,5, respectively; iqr = 0) towards the higher level of the scale. As for the SMNVC, out of 13 people, only 2 participants chose VS5 and values for confidence (mdn = 5, iqr = 1), comfort (mdn = 4, iqr = 1), enjoyability (mdn = 4, iqr = 1) and desire (mdn = 4, iqr = 1) were centered towards the higher level of the scale. No participants reported VS1 in SMNVC.

In *fixed-FoV*, most participants (11, out of 19) chose VS5, and 6 of them with the highest degree of confidence (mdn = 6, iqr = 2). For these 11 participants, most (6 and 3) reported comfort (mdn = 2; iqr = 0.5) and enjoyability (mdn = 3, iqr = 3) towards the lower level of the scale, but most responses (3) for future desire were centered (mdn = 3, iqr = 2.5). Although 12 participants reported SMNVC, no participants chose VS5.

5.3 Objective Measures

To understand user behaviour when viewing 360° video, we started by mapping yaw, roll, and pitch values caused by head movement to time. No visual differences were found between conditions and expected behaviours (e.g. more variation of yaw due to looking from side-to-side) were consistent across conditions. Longitude and latitude corresponding to the central axis of head direction were mapped to hotspot maps (see supplementary material for video of hotspots by condition), using Getis-Ord Gi* at a confidence interval of 95%. Based on this video, we made notes of user behaviour and possible divergence between conditions. For brevity, we present only some behaviours/observations. During stationary shots or shots with little movement, participants explored the scene leading to the creation of multiple clusters. During scenes with translation movement like flying, participants created clusters on the direction of the movement and respected the shape of the environment. For example, in I_{24}, when flying through the canyons, a cluster formed on the canyon direction and in the shape of the canyon opening, but as the pilot left the mountain and space opened up, participants explored, creating multiple clusters. Scene changes led to exploratory behaviour if a new point of interest was not present. For example, I_8 to I_{10}, had points of interest in the same position, so even as the scene changed, clusters remained, but the transition to I_{11} led to participants looking for a new point of interest. Participants were reactive to audio cues (e.g. I_{12} looking to see who was talking) and visual cues (e.g. I_{15} looking at the highlighted path). No discernible differences were found across conditions.

5.3.1 Accumulated Angles. Regarding accumulated angles across the video and intervals classified automatically or manually, several significant differences were found. Only significant differences are reported and all post-hoc paired comparisons were adjusted with Holm-Bonferroni correction. Considering the full video:

- For the **full population**, F(2,44) = 4.772, p = 0.013, a significant difference (p = 0.024) was found between *fixed-FoV* (11974 ± 631.7) and *unrestricted-FoV* (14332 ± 847.4), but not with *dynamic-FoV* (13793 ± 910.4).
- For the **75th upper percentile subpopulation**, F(2,28) = 3.626, p = 0.05, a significant difference (p = 0.049) was found between *fixed-FoV* (12398 ± 835.1) and *unrestricted-FoV* (13958 ± 859.7), but not with *dynamic-FoV* (12518 ± 1079).

For the **full population** and considering the automatic classification of movement:

- For when there is camera movement, F(2,44) = 4.364, p = 0.019, a significant difference (p = 0.021) was found between *fixed-FoV* (7867 ± 398.9) and *unrestricted-FoV* (8878 ± 509.3), but not with *dynamic-FoV* (8288 ± 503.7).
- For when the camera is stationary, F(2,44) = 4.174, p = 0.022, a significant difference (p = 0.05) was found between *fixed-FoV* (4653 ± 369.8) and *unrestricted-FoV* (5453 ± 377.2), but not with *dynamic-FoV* (5349 ± 272.2).

For the **full population** and considering the manual classification of movement:

- Joining intervals classified as "fast" or "slow", F(2,44) = 3.984, p = 0.026, a significant difference (p = 0.033) was found between *fixed-FoV* (7480 ± 399.5) and *unrestricted-FoV* (8792 ± 513.5), but not with *dynamic-FoV* (8265 ± 501.8).
- For intervals classified as "slow", F(2,44) = 4.479, p = 0.017, a significant difference (p = 0.003) was found between *fixed-FoV* (2335 ± 170.7) and *unrestricted-FoV* (2776 ± 172.2), but not with *dynamic-FoV* (2537 ± 121.3).
- For intervals classified as "stationary", F(2,44) = 4.825, p = 0.013, a significant difference (p = 0.05) was found between *fixed-FoV* (4486 ± 278.8) and *unrestricted-FoV* (5540 ± 375.5), but not with *dynamic-FoV* (5325 ± 278.8).

For the **upper 75th percentile subpopulation** and considering the automatic classification of movement:

- For when there is camera movement, F(2,28) = 4.731, p = 0.017, a significant difference (p = 0.021) was found between *fixed-FoV* (7600 ± 570.2) and *unrestricted-FoV* (8874 ± 554.3), but not with *dynamic-FoV* (7545 ± 650.2).
- For when the camera is stationary, F(2,28) = 4.559, p = 0.019, a significant difference (p = 0.05) was found between *dynamic-FoV*(4070 ± 207.1) and *unrestricted-FoV* (5084 ± 366), but not with *fixed-FoV* (4643 ± 252.3).

For the **upper 75th percentile subpopulation** and considering the manual classification of movement:

- Joining intervals classified as "fast" or "slow", F(2,28) = 4.153, p = 0.026, a significant difference (p = 0.03) was found between *fixed-FoV* (7557 ± 569.6) and *unrestricted-FoV* (8769 ± 557.9), but not with *dynamic-FoV* (7519 ± 651.3).
- For intervals classified as "slow", F(2,28) = 4.479, p = 0.017, a significant difference (p = 0.018) was found between *fixed-FoV* (2180 ± 187.1) and *unrestricted-FoV* (2775 ± 176.6), but not with *dynamic-FoV* (2483 ± 167.5).
- For intervals classified as "stationary", F(2,28) = 3.326, p = 0.05, a significant difference (p = 0.05) was found between *fixed-FoV* (4689 ± 253.4) and *unrestricted-FoV* (5188 ± 368.8), but not with *dynamic-FoV* (4435 ± 290.4).

5.3.2 FoV size in dynamic-FoV. To understand how FoV size varied in *dynamic-FoV*, we looked at mean values and standard errors for the automatic and manual classification of locomotion. For the automatic classification, when there was camera movement, the mean FoV size was 64.64 ± 0.6307, increasing to 87.49 ± 0.02536 when stationary. The mean value is not exactly 90º due to changes in value when transitioning between classifications. For the manual classification, in intervals classified as "stationary", the mean value was 86.93 ± 0.02239, being consistent with the automatic classification. However, when comparing intervals classified as "slow" (81.28 ± 0.3638) and "fast" (57.64 ± 0.8187) it is possible to understand that most restriction happens during these "fast" intervals. When joining intervals

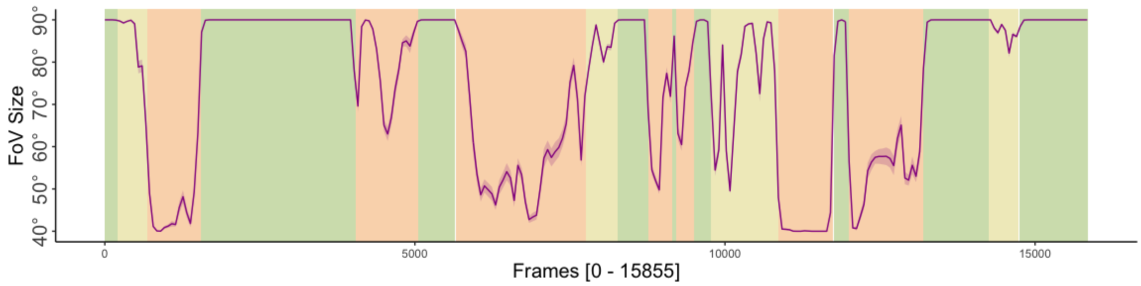

Fig. 4. Mean FoV size for *dynamic-FoV* across time, using a binning of 2 seconds. Colors show the manual classifications of the motion in each time interval (Green: "stationary"; yellow: "slow"; orange: "fast")

with "slow" and "fast" movement, the mean value (64.16 ± 0.6402) is similar to the one found for the automatic classification. Fig. 4 maps mean FoV size to time in *dynamic-FoV*; a stricter FoV restriction was clearly applied to "fast" intervals, while "slow" intervals offer more variation in values.

5.4 Thematic Analysis

Coded segments were grouped into six main themes: Experience (how they felt about the experience), Task (how they engaged with the story), Content (opinions on the 360° video), Comfort (how they felt during the experience including physical symptoms reported), Immersion/Presence (elements that broke the immersion of the 360° video), and Perceived Visual Modifications (visual changes noticed). For brevity, we will not extensively describe them but will synthesize relevant information on the use of *dynamic-FoV* and *fixed-FoV*.

Regarding *dynamic-FoV*, participants reported mixed opinions (e.g. P1 "I think it was something unnatural. For me, the objective of using a headset is to see the things around you. Since I don't feel sick while being able to see everything, having a black spot covering half of the screen is a bit useless. Then, I found it annoying that it would adjust. It's adding more visible movement than what was there before.", P23 "I was conscious of it, that it was happening, that it wasn't completely natural, but I don't feel like it was distracting or made the experience uncomfortable."). Several participants considered *dynamic-FoV* to be part of the experience, often referring to it as a focus (e.g. P6 "I think that the part where the field of view gets reduced makes sense, because when we are going fast, the eye tries to focus. I think that makes sense.", P2 "I think I was more focused. Since I had more vision, I would focus more on that part. Then, I would move around, and it would focus where I was looking at.", P12 "It made sense to me when it's accelerating, because of the speed, as when a person's going fast, they're focusing on the target and don't give much attention to their peripheral vision. There it worked well.", P7 "It forced me to focus on the point where there was movement, so I think it helped during the experience"). However, for some participants the *dynamic-FoV* caused confusion (e.g. P21 "When it did that, I felt like taking a step back, when it closed. Or I was trying to move away from that effect, or that I was taking a step forward and felt unbalanced.") and some did not understand why the effect happened (e.g. P15 thought that the FoV was being changed by the researcher).

For *fixed-FoV*, several participants expressed frustration for its existence (e.g. P19 "More than too distracting, I felt like I was losing a lot of information, by not seeing the surroundings. Also, because, if you have this video in the middle of beautiful mountains, and you just can see one tiny bit.", P4 "I interacted less this time, and still felt sick.", P7 "This one was always closed, it was like looking at a TV screen, I didn't feel as present."). Some participants counteracted the fear of missing out by moving more (e.g. P1 "I couldn't read everything that was on screen. For example, for the name of the documentary, in the beginning, I had to move my head from one side to the other to be able to read it."). It is also relevant to point out that several participants reported eye discomfort (e.g. P19 "I noticed there is a bigger difference in brightness, and maybe that is why my eyes feel weird when I take off the VR headset", P13 "I felt my eyes blinking more.").

For *unrestricted-FoV*, several participants reported using the wider FoV to explore the scene (e.g. P22 "In the others, since the field of view was smaller, it was good to focus on that determinate thing, but here, since it didn't have that, there was more freedom to look around."). However, they also reported discomfort, specifically in scenes with fast movement (e.g. P18 "I felt uncomfortable when they were going down the canyon because the objects moved really fast and they seemed really close to me.", P16 "There were some moments when going through the narrow canyons, for example, I noticed the feeling of vertigo a bit more.").

6 DISCUSSION

Our study demonstrated the efficacy of the *dynamic-FoV* in the mitigation of VIMS symptoms. *Dynamic-FoV* was shown to be statistically effective in reducing/maintaining scores of SSQ-TS, SSQ-N, VRSQ-TS, and VRSQ-D when compared to *unrestricted-FoV*, for both the full population and upper 75th percentile subpopulation. Likewise, *fixed-FoV* was shown to be statistically effective in reducing/maintaining scores of SSQ-D, VRSQ-TS and VRSQ-D compared to *unrestricted-FoV*, for the full population and upper 75th percentile subpopulation. No differences were found between *dynamic-FoV* and *fixed-FoV*; this is expected as the FoV size of *dynamic-FoV* during "fast" intervals (see Fig. 4) is close to the FoV size of *fixed-FoV* (40°), therefore blocking peripheral optical flow more prevalent in those intervals (see Fig. 2). The behaviour of participants for "fast" intervals in *dynamic-FoV*, *fixed-FoV* and *unrestricted-FoV* is similar, as based on the cluster formation in heatmaps and no significant differences in the amount of movement (whereas all other intervals were significant). Therefore, participants experiencing *unrestricted-FoV* were likely to be affected by high values of peripheral optical flow. This is also confirmed by P18 and P16 statements on discomfort in *unrestricted-FoV*. Finally, its also worthy of note that participants for *fixed-FoV* reported oculomotor symptoms, as well as in the semi-structured interviews reporting eye discomfort (e.g. P19, P13); although we cannot conclude a cause, we posit that the severe FoV restriction for a long period of time might cause eye fixation leading to eye strain. The severity of simulator sickness symptoms typically increases with time [37]. For example, Min et al. [74] prompted users operating a driving simulator with an oral SSQ at 5-minute intervals; participants reported nausea and disorientation after 10 minutes and oculomotor symptoms after 25 minutes. Due to a lack of availability of longer 360° videos [32, 79], we exposed users to relatively short stimuli of 8'49" minutes (less than the reported mean of 10 minutes [98]). The low SSQ-TS and SSQ-O scores we observed are consistent with this reduced exposure time and higher values may result from longer exposures. Our current results should be interpreted with this caveat in mind and future work should explore the use of a longer exposure time. We believe this would be particularly valuable as it may exacerbate the differences between conditions.

Considering presence items, as expected, participants experiencing *unrestricted-FoV* reported higher values for general presence and spatial presence compared to *fixed-FoV*. This relationship is expected, since more severe FoV restriction has been shown to reduce the sense of presence [3, 41]. Based on the statistically significant differences in accumulated angles over several types of locomotion, we conclude that participants in *fixed-FoV* moved their head less than in *unrestricted-FoV*, which may explain the reduced spatial presence values for *fixed-FoV*. However, we note that in the semi-structured interviews, some participants reported trying to use motions to mitigate the limitations of the *fixed-FoV* (e.g. P1 moving their head to read the video title).

Although presence items were not significantly different for *dynamic-FoV*, mean scores were higher than for *fixed-FoV*, and involvement was higher than for *unrestricted-FoV* as well. This supports further development of our *dynamic-FoV*. FoV restriction is a noticeable effect, as seen by Fig. 3 and by the statistical significance for VS1 and VS5. First off, the quantity of visual statements is intended to identify the most noticeable changes (by introducing statements that exist regardless of the condition) but the wording is subjective to users; for example, some users identified the FoV restriction as part of "virtual environment" in VS1, which leads to differences between VS1 and VS5. Being noticeable is not necessarily bad, as participants in the MNVC and SMNVC reported these statement's enjoyability and comfort towards the central or higher levels of the scale. However, their desire for its future inclusion is more diverse in their responses. Looking at semi-structured interviews can help clarify this disagreement. For some participants (e.g. P2, P6, P7, P12), the *dynamic-FoV* was considered as part of the experience or as an attention guidance mechanism, especially in intervals with "fast" movement. Unintentionally, *dynamic-FoV* can work as attention guidance since the point of interest in a scene is many times something that causes optical flow. For example, when the secondary pilot jumps in I_{22}, the point of interest is the lead pilot, an element that causes more optical flow through its movement, than looking at the faraway trees. FoV restriction when transitioning to a "fast" interval can also seem like it is intentional. For example, when the pilots are preparing to jump, there is little optical flow noise and subsequently a small FoV restriction; as they jump and transition to the "fast" interval, the FoV restriction is increased to its minimum value of 40º, making it seem like it was intentionally introduced by the video. For other participants, the *dynamic-FoV* was seen as something that was distracting and not helpful, as stated by P1 "It's adding more visible movement than what was there before". Contemplating on Fig. 4, we posit that in "slow" intervals, changes to FoV size might introduce optical flow due to the contraction of the FoV restriction, making it more noticeable for users. Current results should be interpreted having in mind the FoV size limits used. While our inner FoV diameter of 40º is smaller than Fernandes and Feiner's 50º [41], it is of note that our restriction of dynamic-FoV is mostly applied to "fast" intervals (from the comparison of mean FoV sizes and Fig. 4) and that in those intervals the mean FoV size (57.64º) is higher than 40º. Since stricter FoV restrictions can affect both SSQ and presence scores [3, 41], future studies should investigate and adjust the minimum FoV size accordingly, with the goal of maximizing presence and minimizing symptoms.

6.1 Implications for Design, Limitations and Future Work

Aligning peripheral optical flow with motion classification for *dynamic-FoV* has shown to be effective in mitigating VIMS, while maintaining presence. Although noticeable, *dynamic-FoV* was well accepted by participants, allowing for exploration of "stationary" and "slow" scenes, and protecting the user from optical flow during "fast" scenes. While some participants enjoyed the *dynamic-FoV* considering it to be intentional, some participants found it to be distracting due to instability in FoV size. Previous work [18] has suggested that vection change like the one caused by the FoV expanding and contracting alternately can lead to exacerbated symptoms. While we try to reduce this instability by polling optical flow ahead of time and smooth dampening the size of FoV, these attempts are not fruitful in "slow" intervals. The crux of the issue, in this case, is when should you protect the user: a fast response to optical flow stimuli can cause FoV instability if the optical flow stimuli is not maintained; a slow response to optical flow stimuli can expose the user to the stimuli for far longer than needed.

A possible solution using motion classification involves having automatic classification between "slow" scenes with small rotational or translational movement and "fast" scenes with considerable translational movement. This classification would allow for restricted FoV to be applied only in "fast" scenes, to customize parameters like the time of response to the type of scene, or to customize VIMS mitigation strategies to the type of scene (e.g. using a less obtrusive strategy in "slow" scenes). Future work on velocity estimation or simultaneous localization using OpenVSLAM could introduce a plethora of opportunities to augment 360° video. While this is not yet possible for videos with multiple scenes due to inconsistencies in measures, single-shot videos can be used. For example, based on the precomputed locomotion direction of a single-shot video, we could guide attention towards the direction of movement prior to it happening.

Regarding limitations of our work, while we present a study with only one video, the diversity of scenes it includes (different speeds, different camera placements, computer-generated scenes, scenes with special effects, etc.) are positive for the generalization of our *dynamic-FoV* pipeline for other videos. Future studies should focus on the validation of the pipeline in different types of videos in order to determine the video characteristics that are most suitable for dynamic FoV manipulation. Furthermore, our dynamic-FoV pipeline is only responsive to the optical flow of the content and ignores optical flow created by the user from translation and rotation. Future implementations of our pipeline would benefit from incorporating user behaviour data, such as head dispersion as reported by Lim et al [63]. Our results are usable by other researchers and highlight the importance of a mixed-methods approach (using self-reported data, objective measures, and semi-structured interviews) to analyze a complex topic such as VIMS.

7 CONCLUSION

In this paper, we presented a novel strategy for VIMS reduction in 360° video using peripheral optical flow and movement classification from Visual SLAM, both unexplored in the context of 360° video, to dynamically restrict FoV, blocking the peripheral optical flow that exacerbates VIMS symptoms. We evaluated our technique through a within-subjects study (N=23) comparing our design candidate (*dynamic-FoV*) to two baselines (*unrestricted-FoV* and *fixed-FoV*). Our findings show the effectiveness of *dynamic-FoV* in mitigating VIMS, while maintaining presence. Future work for generalizing our system is promising, and could help make VR accessible for all.

ACKNOWLEDGMENTS

We would like to thank Dina Dionísio and Rui Trindade who helped with data collection. This work has been supported by MITIExcell (M1420-01-0145-FEDER-000002), MADEIRA 14-20 FEDER funded project Beanstalk (2015-2020), LARSyS-FCT Pluriannual funding 2020-2023 (UIDB/50009/2020) and FCT Ph.D. Grant PD/BD/128330/2017.

REFERENCES

[1] 2017. Tunneling Demo | Google VR. https://developers.google.com/vr/elements/tunneling

[2] Isayas Berhe Adhanom, Nathan Navarro Griffin, Paul MacNeilage, and Eelke Folmer. 2020. The Effect of a Foveated Field-of-view Restrictor on VR Sickness. In *2020 IEEE Conference on Virtual Reality and 3D User Interfaces (VR)*. 645–652. https://doi.org/10.1109/VR46266.2020.00087 ISSN: 2642-5254.

[3] Majed Al Zayer, Isayas B. Adhanom, Paul MacNeilage, and Eelke Folmer. 2019. The Effect of Field-of-View Restriction on Sex Bias in VR Sickness and Spatial Navigation Performance. In *Proceedings of the 2019 CHI Conference on Human Factors in Computing Systems (CHI '19)*. ACM, New York, NY, USA, 354:1–354:12. https://doi.org/10.1145/3290605.3300584

[4] Shelly L. Ames, James S. Wolffsohn, and Neville A. Mcbrien. 2005. The Development of a Symptom Questionnaire for Assessing Virtual Reality Viewing Using a Head-Mounted Display:. *Optometry and Vision Science* 82, 3 (March 2005), 168–176. https://doi.org/10.1097/01.OPX.0000156307.95086.6

[5] Samuel Ang and John Quarles. 2020. GingerVR: An Open Source Repository of Cybersickness Reduction Techniques for Unity. In *2020 IEEE Conference on Virtual Reality and 3D User Interfaces Abstracts and Workshops (VRW)*. IEEE, Atlanta, GA, USA, 460–463. https://doi.org/10.1109/VRW50115.2020.00097

[6] Simon Baker and Iain Matthews. 2004. Lucas-Kanade 20 Years On: A Unifying Framework. *International Journal of Computer Vision* 56, 3 (Feb. 2004), 221–255. https://doi.org/10.1023/B:VISI.0000011205.11775.fd

[7] Paulo Bala, Raul Masu, Valentina Nisi, and Nuno Nunes. 2019. "When the Elephant Trumps": A Comparative Study on Spatial Audio for Orientation in 360º Videos. In *Proceedings of the 2019 CHI Conference on Human Factors in Computing Systems - CHI '19*. ACM Press, Glasgow, Scotland Uk, 1–13. https://doi.org/10.1145/3290605.3300925

[8] Paulo Bala, Ian Oakley, Valentina Nisi, and Nuno Nunes. 2020. Staying on Track: a Comparative Study on the Use of Optical Flow in 360° Video to Mitigate VIMS. In *ACM International Conference on Interactive Media Experiences*. ACM, Cornella, Barcelona Spain, 82–93. https://doi.org/10.1145/3391614.3393658

[9] Tarik Benbrahim. 2019. GoPro x RYOT: Tales From the Edge in 4K VR | Jeb Corliss. https://www.youtube.com/watch?v=szHgpgVzfMM&ab_channel=GoPro

[10] María Carolina Bermúdez Rey, Torin K. Clark, Wei Wang, Tania Leeder, Yong Bian, and Daniel M. Merfeld. 2016. Vestibular Perceptual Thresholds Increase above the Age of 40. *Frontiers in Neurology* 7 (Oct. 2016). https://doi.org/10.3389/fneur.2016.00162

[11] A. Berthoz, B. Pavard, and L. R. Young. 1975. Perception of linear horizontal self-motion induced by peripheral vision (linearvection) basic characteristics and visual-vestibular interactions. *Experimental Brain Research* 23, 5 (Nov. 1975), 471–489.

[12] Chris Bevan and David Green. 2018. A Mediography of Virtual Reality Non-Fiction: Insights and Future Directions. In *Proceedings of the 2018 ACM International Conference on Interactive Experiences for TV and Online Video - TVX '18*. ACM Press, SEOUL, Republic of Korea, 161–166. https://doi.org/10.1145/3210825.3213557

[13] Chris Bevan, David Philip Green, Harry Farmer, Mandy Rose, Kirsten Cater, Danaë Stanton Fraser, and Helen Brown. 2019. Behind the Curtain of the "Ultimate Empathy Machine": On the Composition of Virtual Reality Nonfiction Experiences. In *Proceedings of the 2019 CHI Conference on Human Factors in Computing Systems - CHI '19*. ACM Press, Glasgow, Scotland Uk, 1–12. https://doi.org/10.1145/3290605.3300736

[14] Jiwan Bhandari, Paul MacNeilage, and Eelke Folmer. 2018. Teleportation without Spatial Disorientation Using Optical Flow Cues. In *Proceedings of the 44th Graphics Interface Conference* (Toronto, Canada) *(GI '18)*. Canadian Human-Computer Communications Society, Waterloo, CAN, 162–167. https://doi.org/10.20380/GI2018.22

[15] Roger Bivand, L. Anselin, O. Berke, A. Bernat, M. Carvalho, Y. Chun, C. F. Dormann, S. Dray, R. Halbersma, and N. Lewin-Koh. 2011. *spdep: Spatial dependence: weighting schemes, statistics and models*. R package version 0.5-31, URL http://CRAN. R-project. org/package= spdep.

[16] Roger Bivand, Tim Keitt, Barry Rowlingson, and E. Pebesma. 2014. rgdal: Bindings for the geospatial data abstraction library. *R package version 0.8-16* (2014).

[17] Mark Bolas, J. Adam Jones, Ian McDowall, and Evan Suma. 2017. Dynamic field of view throttling as a means of improving user experience in head mounted virtual environments.

[18] Frederick Bonato, Andrea Bubka, Stephen Palmisano, Danielle Phillip, and Giselle Moreno. 2008. Vection Change Exacerbates Simulator Sickness in Virtual Environments. *Presence: Teleoperators and Virtual Environments* 17, 3 (June 2008), 283–292. https://doi.org/10.1162/pres.17.3.283

[19] Jelte E. Bos, Sjoerd C. de Vries, Martijn L. van Emmerik, and Eric L. Groen. 2010. The effect of internal and external fields of view on visually induced motion sickness. *Applied Ergonomics* 41, 4 (July 2010), 516–521. https://doi.org/10.1016/j.apergo.2009.11.007

[20] G. Bradski. 2000. The OpenCV Library. *Dr. Dobb's Journal of Software Tools* (2000).

[21] Th. Brandt, Johannes Dichgans, and Ed Koenig. 1973. Differential effects of central versus peripheral vision on egocentric and exocentric motion perception. *Experimental Brain Research* 16, 5 (March 1973), 476–491. https://doi.org/10.1007/BF00234474

[22] Virginia Braun and Victoria Clarke. 2006. Using thematic analysis in psychology. *Qualitative research in psychology* 3, 2 (2006), 77–101.

[23] Pulkit Budhiraja, Mark Roman Miller, Abhishek K. Modi, and David Forsyth. 2017. Rotation Blurring: Use of Artificial Blurring to Reduce Cybersickness in Virtual Reality First Person Shooters. *arXiv:1710.02599 [cs]* (Oct. 2017). http://arxiv.org/abs/1710.02599 arXiv: 1710.02599.

[24] Helmut Buhler, Sebastian Misztal, and Jonas Schild. 2018. Reducing VR Sickness Through Peripheral Visual Effects. In *2018 IEEE Conference on Virtual Reality and 3D User Interfaces (VR)*. IEEE, Reutlingen, 517–9. https://doi.org/10.1109/VR.2018.8446346

[25] Fabio Buttussi and Luca Chittaro. 2019. Locomotion in Place in Virtual Reality: A Comparative Evaluation of Joystick, Teleport, and Leaning. *IEEE Transactions on Visualization and Computer Graphics* (2019), 1–1. https://doi.org/10.1109/TVCG.2019.2928304

[26] S. van Buuren and Karin Groothuis-Oudshoorn. 2010. mice: Multivariate imputation by chained equations in R. *Journal of statistical software* (2010), 1–68. Publisher: University of California, Los Angeles.

[27] Zekun Cao, Jason Jerald, and Regis Kopper. 2018. Visually-Induced Motion Sickness Reduction via Static and Dynamic Rest Frames. In *2018 IEEE Conference on Virtual Reality and 3D User Interfaces (VR)*. 105–112. https://doi.org/10.1109/VR.2018.8446210

[28] David Caruso, Jakob Engel, and Daniel Cremers. 2015. Large-scale direct SLAM for omnidirectional cameras. In *2015 IEEE/RSJ International Conference on Intelligent Robots and Systems (IROS)*. IEEE, Hamburg, Germany, 141–148. https://doi.org/10.1109/IROS.2015.7353366

[29] Eunhee Chang, Hyun Taek Kim, and Byounghyun Yoo. 2020. Virtual Reality Sickness: A Review of Causes and Measurements. *International Journal of Human–Computer Interaction* (July 2020), 1–25. https://doi.org/10.1080/10447318.2020.1778351

[30] Shih-Han Chou, Cheng Sun, Wen-Yen Chang, Wan-Ting Hsu, Min Sun, and Jianlong Fu. 2020. 360-Indoor: Towards Learning Real-World Objects in 360º Indoor Equirectangular Images. In *The IEEE Winter Conference on Applications of Computer Vision*. 845–853.

[31] Rudolph P. Darken, William R. Cockayne, and David Carmein. 1997. The omni-directional treadmill: a locomotion device for virtual worlds. In *Proceedings of the 10th annual ACM symposium on User interface software and technology - UIST '97*. ACM Press, Banff, Alberta, Canada, 213–221. https://doi.org/10.1145/263407.263550

[32] Erwan J. David, Jesús Gutiérrez, Antoine Coutrot, Matthieu Perreira Da Silva, and Patrick Le Callet. 2018. A dataset of head and eye movements for 360° videos. In *Proceedings of the 9th ACM Multimedia Systems Conference*. ACM, Amsterdam Netherlands, 432–437. https://doi.org/10.1145/

3204949.3208139

[33] Simon Davis, Keith Nesbitt, and Eugene Nalivaiko. 2015. Comparing the onset of cybersickness using the Oculus Rift and two virtual roller coasters. In *Proceedings of the 11th Australasian Conference on Interactive Entertainment (IE 2015)*, Vol. 27. 30. http://crpit.com/confpapers/CRPITV167Davis.pdf

[34] M. H. Draper, E. S. Viire, T. A. Furness, and V. J. Gawron. 2001. Effects of image scale and system time delay on simulator sickness within head-coupled virtual environments. *Human Factors* 43, 1 (2001), 129–146. https://doi.org/10.1518/001872001775992552

[35] Henry Been-Lirn Duh, Donald E. Parker, and Thomas A. Furness. 2001. An "Independent Visual Background" Reduced Balance Disturbance Envoked by Visual Scene Motion: Implication for Alleviating Simulator Sickness. In *Proceedings of the SIGCHI Conference on Human Factors in Computing Systems* (Seattle, Washington, USA) *(CHI '01)*. Association for Computing Machinery, New York, NY, USA, 85–89. https://doi.org/10.1145/365024.365051

[36] Henry Been-Lirn Duh, Donald E. Parker, and Thomas A. Furness. 2004. An Independent Visual Background Reduced Simulator Sickness in a Driving Simulator. *Presence: Teleoperators and Virtual Environments* 13, 5 (Oct. 2004), 578–588. https://doi.org/10.1162/1054746042545283

[37] Natalia Dużmańska, Paweł Strojny, and Agnieszka Strojny. 2018. Can Simulator Sickness Be Avoided? A Review on Temporal Aspects of Simulator Sickness. *Frontiers in Psychology* 9 (Nov. 2018). https://doi.org/10.3389/fpsyg.2018.02132

[38] Sheldon M. Ebenholtz. 2001. *Oculomotor systems and perception.* Cambridge University Press, New York.

[39] Yasin Farmani and Robert J. Teather. 2018. Viewpoint Snapping to Reduce Cybersickness in Virtual Reality. (2018), 168 – 175. https://doi.org/10.20380/GI2018.23

[40] Gunnar Farnebäck. 2003. Two-frame motion estimation based on polynomial expansion. *Image analysis* (2003), 363–370.

[41] Ajoy S Fernandes and Steven K. Feiner. 2016. Combating VR sickness through subtle dynamic field-of-view modification. In *2016 IEEE Symposium on 3D User Interfaces (3DUI)*. IEEE, Greenville, SC, USA, 201–210. https://doi.org/10.1109/3DUI.2016.7460053

[42] Andy Field, Jeremy Miles, and Zoë Field. 2012. *Discovering statistics using R.* Sage publications.

[43] Eivind Flobak, Jo D. Wake, Joakim Vindenes, Smiti Kahlon, Tine Nordgreen, and Frode Guribye. 2019. Participatory Design of VR Scenarios for Exposure Therapy. In *Proceedings of the 2019 CHI Conference on Human Factors in Computing Systems - CHI '19*. ACM Press, Glasgow, Scotland Uk, 1–12. https://doi.org/10.1145/3290605.3300799

[44] Sebastian Freitag, Benjamin Weyers, and Torsten W. Kuhlen. 2017. Assisted travel based on common visibility and navigation meshes. In *2017 IEEE Virtual Reality (VR)*. IEEE, 369–370. https://doi.org/10.1109/VR.2017.7892330

[45] Jann Philipp Freiwald, Oscar Ariza, Omar Janeh, and Frank Steinicke. 2020. Walking by Cycling: A Novel In-Place Locomotion User Interface for Seated Virtual Reality Experiences. In *Proceedings of the 2020 CHI Conference on Human Factors in Computing Systems*. ACM, Honolulu HI USA, 1–12. https://doi.org/10.1145/3313831.3376574

[46] Augusto Garcia-Agundez, Aiko Westmeier, Polona Caserman, Robert Konrad, and Stefan Göbel. 2017. An Evaluation of Extrapolation and Filtering Techniques in Head Tracking for Virtual Environments to Reduce Cybersickness. In *Serious Games (Lecture Notes in Computer Science)*. Springer, Cham, 203–211. https://doi.org/10.1007/978-3-319-70111-0_19

[47] John F Golding. 1998. Motion sickness susceptibility questionnaire revised and its relationship to other forms of sickness. *Brain Research Bulletin* 47, 5 (Nov. 1998), 507–516. https://doi.org/10.1016/S0361-9230(98)00091-4

[48] Google. 2020. Google Earth VR. https://arvr.google.com/earth/

[49] John W. Graham. 2009. Missing Data Analysis: Making It Work in the Real World. *Annual Review of Psychology* 60, 1 (Jan. 2009), 549–576. https://doi.org/10.1146/annurev.psych.58.110405.085530

[50] Jože Guna, Gregor Geršak, Iztok Humar, Jeungeun Song, Janko Drnovšek, and Matevž Pogačnik. 2019. Influence of video content type on users' virtual reality sickness perception and physiological response. *Future Generation Computer Systems* 91 (Feb. 2019), 263–276. https://doi.org/10.1016/j.future.2018.08.049

[51] Kelly S. Hale and Kay M. Stanney (Eds.). 2014. *Handbook of Virtual Environments: Design, Implementation, and Applications, Second Edition* (0 ed.). CRC Press. https://doi.org/10.1201/b17360

[52] Haikun Huang, Michael Solah, Dingzeyu Li, and Lap-Fai Yu. 2019. Audible Panorama: Automatic Spatial Audio Generation for Panorama Imagery. In *Proceedings of the 2019 CHI Conference on Human Factors in Computing Systems (CHI '19)*. ACM, New York, NY, USA, 621:1–621:11. https://doi.org/10.1145/3290605.3300851

[53] Nupur Kala, Kyungmin Lim, Kwanghyun Won, Jaesung Lee, Tammy Lee, Sehoon Kim, and Wonhee Choe. 2017. P-218: An Approach to Reduce VR Sickness by Content Based Field of View Processing. *SID Symposium Digest of Technical Papers* 48, 1 (May 2017), 1645–1648. https://doi.org/10.1002/sdtp.11956

[54] Shunichi Kasahara, Shohei Nagai, and Jun Rekimoto. 2015. First Person Omnidirectional Video: System Design and Implications for Immersive Experience. In *Proceedings of the ACM International Conference on Interactive Experiences for TV and Online Video* (Brussels, Belgium) *(TVX '15)*. Association for Computing Machinery, New York, NY, USA, 33–42. https://doi.org/10.1145/2745197.2745202

[55] Andras Kemeny, Paul George, Frédéric Mérienne, and Florent Colombet. 2017. New VR Navigation Techniques to Reduce Cybersickness. https://doi.org/10.2352/ISSN.2470-1173.2017.3.ERVR-097

[56] Robert S. Kennedy, Norman E. Lane, Kevin S. Berbaum, and Michael G. Lilienthal. 1993. Simulator Sickness Questionnaire: An Enhanced Method for Quantifying Simulator Sickness. *The International Journal of Aviation Psychology* 3, 3 (July 1993), 203–220. https://doi.org/10.1207/s15327108ijap0303_3

[57] Behrang Keshavarz, Heiko Hecht, and Lisa Zschutschke. 2011. Intra-visual conflict in visually induced motion sickness. *Displays* 32, 4 (Oct. 2011), 181–188. https://doi.org/10.1016/j.displa.2011.05.009

[58] Behrang Keshavarz, Aaron Emile Philipp-Muller, Wanja Hemmerich, Bernhard E. Riecke, and Jennifer L. Campos. 2019. The effect of visual motion stimulus characteristics on vection and visually induced motion sickness. *Displays* 58 (July 2019), 71–81. https://doi.org/10.1016/j.displa.2018.07.005

[59] Hyun K. Kim, Jaehyun Park, Yeongcheol Choi, and Mungyeong Choe. 2018. Virtual reality sickness questionnaire (VRSQ): Motion sickness measurement index in a virtual reality environment. *Applied ergonomics* 69 (2018), 66–73. https://doi.org/10.1016/j.apergo.2017.12.016

[60] Young Youn Kim, Eun Nam Kim, Min Jae Park, Kwang Suk Park, Hee Dong Ko, and Hyun Taek Kim. 2008. The Application of Biosignal Feedback for Reducing Cybersickness from Exposure to a Virtual Environment. *Presence* 17, 1 (Feb. 2008), 1–16. https://doi.org/10.1162/pres.17.1.1

[61] Udo Kuckartz and Stefan Rädiker. 2019. *Analyzing qualitative data with MAXQDA*. Springer.

[62] Joseph J. LaViola, Jr. 2000. A Discussion of Cybersickness in Virtual Environments. *SIGCHI Bull.* 32, 1 (Jan. 2000), 47–56. https://doi.org/10.1145/333329.333344

[63] Kyungmin Lim, Jaesung Lee, Kwanghyun Won, Nupur Kala, and Tammy Lee. 2020. A novel method for VR sickness reduction based on dynamic field of view processing. *Virtual Reality* (July 2020). https://doi.org/10.1007/s10055-020-00457-3

[64] James Jeng-Weei Lin, Habib Abi-Rached, Do-Hoe Kim, Donald E. Parker, and Thomas A. Furness. 2002. A "Natural" Independent Visual Background Reduced Simulator Sickness. *Proceedings of the Human Factors and Ergonomics Society Annual Meeting* 46, 26 (2002), 2124–2128. https://doi.org/10.1177/154193120204602605 arXiv:https://doi.org/10.1177/154193120204602605

[65] Yung-Ta Lin, Yi-Chi Liao, Shan-Yuan Teng, Yi-Ju Chung, Liwei Chan, and Bing-Yu Chen. 2017. Outside-In: Visualizing Out-of-Sight Regions-of-Interest in a 360 Video Using Spatial Picture-in-Picture Previews. In *Proceedings of the 30th Annual ACM Symposium on User Interface Software and Technology*. ACM, 255–265. https://doi.org/10.1145/3126594.3126656

[66] Sean J. Liu, Maneesh Agrawala, Stephen DiVerdi, and Aaron Hertzmann. 2019. View-Dependent Video Textures for 360° Video. In *Proceedings of the 32nd Annual ACM Symposium on User Interface Software and Technology*. ACM, New Orleans LA USA, 249–262. https://doi.org/10.1145/3332165.3347887

[67] Pietro Lungaro, Rickard Sjoberg, Alfredo Jose Fanghella Valero, Ashutosh Mittal, and Konrad Tollmar. 2018. Gaze-Aware Streaming Solutions for the Next Generation of Mobile VR Experiences. *IEEE Transactions on Visualization and Computer Graphics* 24, 4 (April 2018), 1535–1544. https://doi.org/10.1109/TVCG.2018.2794119

[68] Ville Mäkelä, Tuuli Keskinen, John Mäkelä, Pekka Kallioniemi, Jussi Karhu, Kimmo Ronkainen, Alisa Burova, Jaakko Hakulinen, and Markku Turunen. 2019. What Are Others Looking at? Exploring 360° Videos on HMDs with Visual Cues about Other Viewers. In *Proceedings of the 2019 ACM International Conference on Interactive Experiences for TV and Online Video* (Salford (Manchester), United Kingdom) *(TVX '19)*. Association for Computing Machinery, New York, NY, USA, 13–24. https://doi.org/10.1145/3317697.3323351

[69] John W. Mauchly. 1940. Significance Test for Sphericity of a Normal n-Variate Distribution. *The Annals of Mathematical Statistics* 11, 2 (June 1940), 204–209. https://doi.org/10.1214/aoms/1177731915

[70] Mark McGill, Daniel Boland, Roderick Murray-Smith, and Stephen Brewster. 2015. A Dose of Reality: Overcoming Usability Challenges in VR Head-Mounted Displays. In *Proceedings of the 33rd Annual ACM Conference on Human Factors in Computing Systems - CHI '15*. ACM Press, Seoul, Republic of Korea, 2143–2152. https://doi.org/10.1145/2702123.2702382

[71] Mark McGill, Alexander Ng, and Stephen Brewster. 2017. I Am The Passenger: How Visual Motion Cues Can Influence Sickness For In-Car VR. In *Proceedings of the 2017 CHI Conference on Human Factors in Computing Systems (CHI '17)*. ACM, New York, NY, USA, 5655–5668. https://doi.org/10.1145/3025453.3026046

[72] Doug McIlroy, Ray Brownrigg, Thomas P. Minka, and Roger Bivand. 2014. Mapproj: map projections. *R package version* (2014), 1–2.

[73] Michael Meehan, Sharif Razzaque, Mary C. Whitton, and Frederick P. Brooks. 2003. Effect of latency on presence in stressful virtual environments. In *IEEE Virtual Reality, 2003. Proceedings.* IEEE, 141–148. https://doi.org/10.1109/VR.2003.1191132

[74] Byung-Chan Min, Soon-Cheol Chung, Yoon-Ki Min, and Kazuyoshi Sakamoto. 2004. Psychophysiological evaluation of simulator sickness evoked by a graphic simulator. *Applied Ergonomics* 35, 6 (2004), 549 – 556. https://doi.org/10.1016/j.apergo.2004.06.002

[75] Jason D. Moss and Eric R. Muth. 2011. Characteristics of Head-Mounted Displays and Their Effects on Simulator Sickness. *Human Factors: The Journal of the Human Factors and Ergonomics Society* 53, 3 (June 2011), 308–319. https://doi.org/10.1177/0018720811405196

[76] Justin Munafo, Meg Diedrick, and Thomas A. Stoffregen. 2017. The virtual reality head-mounted display Oculus Rift induces motion sickness and is sexist in its effects. *Experimental brain research* 235, 3 (2017), 889–901. https://doi.org/10.1007/s00221-016-4846-7

[77] Richard Musil. 2020. HMD Geometry Database. https://risa2000.github.io/hmdgdb/

[78] Mahdi Nabiyouni and Doug A. Bowman. 2016. A Taxonomy for Designing Walking-based Locomotion Techniques for Virtual Reality. In *Proceedings of the 2016 ACM Companion on Interactive Surfaces and Spaces (ISS Companion '16)*. ACM, New York, NY, USA, 115–121. https://doi.org/10.1145/3009939.3010076

[79] Afshin Taghavi Nasrabadi, Aliehsan Samiei, Anahita Mahzari, Ryan P. McMahan, Ravi Prakash, Mylène C. Q. Farias, and Marcelo M. Carvalho. 2019. A taxonomy and dataset for 360° videos. In *Proceedings of the 10th ACM Multimedia Systems Conference (MMSys '19)*. Association for Computing Machinery, New York, NY, USA, 273–278. https://doi.org/10.1145/3304109.3325812

[80] Luís A. R. Neng and Teresa Chambel. 2010. Get around 360° hypervideo. In *Proceedings of the 14th International Academic MindTrek Conference on Envisioning Future Media Environments - MindTrek '10*. ACM Press, Tampere, Finland, 119. https://doi.org/10.1145/1930488.1930512

[81] Cuong Nguyen, Stephen DiVerdi, Aaron Hertzmann, and Feng Liu. 2017. Vremiere: In-Headset Virtual Reality Video Editing. In *Proceedings of the 2017 CHI Conference on Human Factors in Computing Systems (CHI '17)*. ACM, New York, NY, USA, 5428–5438. https://doi.org/10.1145/3025453.3025675

[82] Thinh Nguyen-Vo, Bernhard E. Riecke, and Wolfgang Stuerzlinger. 2018. Simulated Reference Frame: A Cost-Effective Solution to Improve Spatial Orientation in VR. In *2018 IEEE Conference on Virtual Reality and 3D User Interfaces (VR)*. IEEE, Reutlingen, 415–422. https://doi.org/10.1109/VR.2018.8446383

[83] Guangyu Nie, Yue Liu, and Yongtian Wang. 2017. [POSTER] Prevention of Visually Induced Motion Sickness Based on Dynamic Real-Time Content-Aware Non-salient Area Blurring. In *2017 IEEE International Symposium on Mixed and Augmented Reality (ISMAR-Adjunct)*. IEEE, Nantes, France, 75–78. https://doi.org/10.1109/ISMAR-Adjunct.2017.35

[84] Nahal Norouzi, Gerd Bruder, and Greg Welch. 2018. Assessing vignetting as a means to reduce VR sickness during amplified head rotations. In *Proceedings of the 15th ACM Symposium on Applied Perception (SAP '18)*. Association for Computing Machinery, New York, NY, USA, 1–8. https://doi.org/10.1145/3225153.3225162

[85] Oculus. 2020. Locomotion | Oculus Developers. https://developer.oculus.com/learn/bp-locomotion/

[86] Amy Pavel, Björn Hartmann, and Maneesh Agrawala. 2017. Shot Orientation Controls for Interactive Cinematography with 360 Video. In *Proceedings of the 30th Annual ACM Symposium on User Interface Software and Technology*. ACM, Québec City QC Canada, 289–297. https://doi.org/10.1145/3126594.3126636

[87] Edzer Pebesma. 2018. Simple Features for R: Standardized Support for Spatial Vector Data. *The R Journal* 10, 1 (2018), 439–446. https://doi.org/10.32614/RJ-2018-009

[88] Yi-Hao Peng, Carolyn Yu, Shi-Hong Liu, Chung-Wei Wang, Paul Taele, Neng-Hao Yu, and Mike Y. Chen. 2020. WalkingVibe: Reducing Virtual Reality Sickness and Improving Realism while Walking in VR using Unobtrusive Head-mounted Vibrotactile Feedback. In *Proceedings of the 2020 CHI Conference on Human Factors in Computing Systems (CHI '20)*. Association for Computing Machinery, New York, NY, USA, 1–12. https://doi.org/10.1145/3313831.3376847

[89] Thiago M. Porcino, Esteban Clua, Daniela Trevisan, Cristina N. Vasconcelos, and Luis Valente. 2017. Minimizing cyber sickness in head mounted display systems: Design guidelines and applications. In *2017 IEEE 5th International Conference on Serious Games and Applications for Health (SeGAH)*. 1–6. https://doi.org/10.1109/SeGAH.2017.7939283

[90] J. D. Prothero, M. H. Draper, T. A. Furness, D. E. Parker, and M. J. Wells. 1999. The use of an independent visual background to reduce simulator side-effects. *Aviation, Space, and Environmental Medicine* 70, 3 Pt 1 (March 1999), 277–283.

[91] R Core Team. 2014. *R: A Language and Environment for Statistical Computing*. R Foundation for Statistical Computing, Vienna, Austria. http://www.R-project.org/

[92] Sharif Razzaque, Zachariah Kohn, and Mary C Whitton. 2001. *Redirected Walking*. Technical Report. University of North Carolina at Chapel Hill, Chapel Hill, NC, USA.

[93] Lisa Rebenitsch and Charles Owen. 2014. Individual Variation in Susceptibility to Cybersickness. In *Proceedings of the 27th Annual ACM Symposium on User Interface Software and Technology (UIST '14)*. ACM, New York, NY, USA, 309–317. https://doi.org/10.1145/2642918.2647394

[94] Lisa Rebenitsch and Charles Owen. 2016. Review on cybersickness in applications and visual displays. *Virtual Reality* 20, 2 (June 2016), 101–125. https://doi.org/10.1007/s10055-016-0285-9

[95] Gary E. Riccio and Thomas A. Stoffregen. 1991. An ecological Theory of Motion Sickness and Postural Instability. *Ecological Psychology* 3, 3 (Sept. 1991), 195–240. https://doi.org/10.1207/s15326969eco0303_2

[96] Sylvia Rothe and Heinrich Hußmann. 2018. Spatial statistics for analyzing data in cinematic virtual reality. In *Proceedings of the 2018 International Conference on Advanced Visual Interfaces - AVI '18*. ACM Press, Castiglione della Pescaia, Grosseto, Italy, 1–3. https://doi.org/10.1145/3206505.3206561

[97] Santeri Saarinen, Ville Mäkelä, Pekka Kallioniemi, Jaakko Hakulinen, and Markku Turunen. 2017. Guidelines for Designing Interactive Omnidirectional Video Applications. In *16th IFIP TC 13 International Conference on Human-Computer Interaction — INTERACT 2017 - Volume 10516*. Springer-Verlag, Berlin, Heidelberg, 263–272. https://doi.org/10.1007/978-3-319-68059-0_17

[98] Dimitrios Saredakis, Ancret Szpak, Brandon Birckhead, Hannah A. D. Keage, Albert Rizzo, and Tobias Loetscher. 2020. Factors Associated With Virtual Reality Sickness in Head-Mounted Displays: A Systematic Review and Meta-Analysis. *Frontiers in Human Neuroscience* 14 (March 2020). https://doi.org/10.3389/fnhum.2020.00096

[99] Thomas Schubert, Frank Friedmann, and Holger Regenbrecht. 2001. The Experience of Presence: Factor Analytic Insights. *Presence: Teleoper. Virtual Environ.* 10, 3 (June 2001), 266–281. https://doi.org/10.1162/105474601300343603

[100] A.F. Seay, D.M. Krum, L. Hodges, and W. Ribarsky. 2001. Simulator sickness and presence in a high FOV virtual environment. In *Proceedings IEEE Virtual Reality 2001*. IEEE Comput. Soc, Yokohama, Japan, 299–300. https://doi.org/10.1109/VR.2001.913806

[101] Volkan Sevinc and Mehmet Ilker Berkman. 2020. Psychometric evaluation of Simulator Sickness Questionnaire and its variants as a measure of cybersickness in consumer virtual environments. *Applied Ergonomics* 82 (Jan. 2020), 102958. https://doi.org/10.1016/j.apergo.2019.102958

[102] Alia Sheikh, Andy Brown, Zillah Watson, and Michael Evans. 2016. Directing attention in 360-degree video. *IET Conference Proceedings* (2016). https://doi.org/10.1049/ibc.2016.0029

[103] Mel Slater and Maria V. Sanchez-Vives. 2016. Enhancing Our Lives with Immersive Virtual Reality. *Frontiers in Robotics and AI* 3 (Dec. 2016). https://doi.org/10.3389/frobt.2016.00074

[104] VERBI Software. 2019. MAXQDA 2020. maxqda.com

[105] Kay M. Stanney, D. Susan Lanham, Robert S. Kennedy, and Robert Breaux. 1999. Virtual Environment Exposure Drop-Out Thresholds. *Proceedings of the Human Factors and Ergonomics Society Annual Meeting* 43, 22 (Sept. 1999), 1223–1227. https://doi.org/10.1177/154193129904302212 Publisher: SAGE Publications Inc.

[106] Anthony Steed, Francisco R. Ortega, Adam S. Williams, Ernst Kruijff, Wolfgang Stuerzlinger, Anil Ufuk Batmaz, Andrea Stevenson Won, Evan Suma Rosenberg, Adalberto L. Simeone, and Aleshia Hayes. 2020. Evaluating immersive experiences during Covid-19 and beyond. *Interactions* 27, 4 (July 2020), 62–67. https://doi.org/10.1145/3406098

[107] Shinya Sumikura, Mikiya Shibuya, and Ken Sakurada. 2019. OpenVSLAM: A Versatile Visual SLAM Framework. In *Proceedings of the 27th ACM International Conference on Multimedia* (Nice, France) *(MM '19)*. ACM, New York, NY, USA, 2292–2295. https://doi.org/10.1145/3343031.3350539

[108] Joel Teixeira and Stephen Palmisano. 2020. Effects of dynamic field-of-view restriction on cybersickness and presence in HMD-based virtual reality. *Virtual Reality* (Aug. 2020). https://doi.org/10.1007/s10055-020-00466-2

[109] Sam Tregillus. 2016. VR-Drop: Exploring the Use of Walking-in-Place to Create Immersive VR Games. In *Proceedings of the 2016 CHI Conference Extended Abstracts on Human Factors in Computing Systems (CHI EA '16)*. ACM, New York, NY, USA, 176–179. https://doi.org/10.1145/2851581.2890374

[110] M. Treisman. 1977. Motion sickness: an evolutionary hypothesis. *Science (New York, N.Y.)* 197, 4302 (July 1977), 493–495. https://doi.org/10.1126/science.301659

[111] Robert J. van Beers, Anne C. Sittig, and Jan J. Denier van der Gon. 1999. Integration of Proprioceptive and Visual Position-Information: An Experimentally Supported Model. *Journal of Neurophysiology* 81, 3 (March 1999), 1355–1364. https://doi.org/10.1152/jn.1999.81.3.1355

[112] Michael Venturino and Maxwell J. Wells. 1990. Head Movements as a Function of Field-of-View Size on a Helmet-Mounted Display. *Proceedings of the Human Factors Society Annual Meeting* 34, 19 (Oct. 1990), 1572–1576. https://doi.org/10.1177/154193129003401932

[113] Nicholas A. Webb and Michael J. Griffin. 2003. Eye movement, vection, and motion sickness with foveal and peripheral vision. *Aviation, space, and environmental medicine* 74, 6 (2003), 622–625. Publisher: Aerospace Medical Association.

[114] David Matthew Whittinghill, Bradley Ziegler, T Case, and B Moore. 2015. Nasum virtualis: A simple technique for reducing simulator sickness. In *Games Developers Conference (GDC)*. 74.

[115] Hadley Wickham. 2009. *ggplot2: Elegant Graphics for Data Analysis*. Springer-Verlag New York. http://ggplot2.org

[116] Carolin Wienrich, Christine Katharina Weidner, Celina Schatto, David Obremski, and Johann Habakuk Israel. 2018. A Virtual Nose as a Rest-Frame - The Impact on Simulator Sickness and Game Experience. In *2018 10th International Conference on Virtual Worlds and Games for Serious Applications (VS-Games)*. IEEE, Wurzburg, 1–8. https://doi.org/10.1109/VS-Games.2018.8493408

[117] Michael Lee Wilson. 2016. The effect of varying latency in a head-mounted display on task performance and motion sickness. (2016).

[118] Robert Xiao and Hrvoje Benko. 2016. Augmenting the Field-of-View of Head-Mounted Displays with Sparse Peripheral Displays. In *Proceedings of the 2016 CHI Conference on Human Factors in Computing Systems - CHI '16* (Santa Clara, California, USA, 2016) *(CHI '16)*. ACM Press, New York, NY, USA, 1221–1232. https://doi.org/10.1145/2858036.2858212

[119] Khalid Yousif, Alireza Bab-Hadiashar, and Reza Hoseinnezhad. 2015. An Overview to Visual Odometry and Visual SLAM: Applications to Mobile Robotics. *Intelligent Industrial Systems* 1, 4 (Dec. 2015), 289–311. https://doi.org/10.1007/s40903-015-0032-7

[120] Daniel Zielasko, Alexander Meißner, Sebastian Freitag, Benjamin Weyers, and Torsten W. Kuhlen. 2018. Dynamic field of view reduction related to subjective sickness measures in an HMD-based data analysis task. In *Proc. of IEEE VR Workshop on Everyday Virtual Reality*.

[121] Daniel Zielasko, Benjamin Weyers, and Torsten W. Kuhlen. 2019. A Non-Stationary Office Desk Substitution for Desk-Based and HMD-Projected Virtual Reality. *2019 IEEE Conference on Virtual Reality and 3D User Interfaces (VR)* (2019), 1884–1889. https://doi.org/10.1109/VR.2019.8797837

Table 4. Full list of abbreviations, acronyms and initialisms

Abbreviation	Original
CSV	Comma Separated Values
d-FoV	dynamic-FoV
ER	Experienced Realism
f-FoV	fixed-FoV
FoV	Field of View
GP	General Presence
HMD	Head Mounted Display
I[1-28]	Interval 1 to 28
INV	Involvement
IPQ	Igroup Presence Questionnaire
MNVC	Most Noticed Visual Change
P[1-23]	Participant 1 to 23
POI	Point of Interest
SLAM	Simultaneous Localization and Mapping
SMNVC	Second Most Noticed Visual Change
SP	Spatial Presence
SSQ	Simulator Sickness Questionnaire
SSQ-D	Disorientation
SSQ-N	Nausea
SSQ-O	OculoMotor
SSQ-TS	Total Severity
u-FoV	unrestricted-FoV
VIMS	Visually Induced Motion Sickness
VO	Visual Odometry
VQ	Visual Questionnaire
VR	Virtual Reality
VRSQ	Virtual Reality Sickness Questionnaire
VRSQ-D	Disorientation
VRSQ-O	OculoMotor
VRSQ-TS	Total Severity
VS	Visual Statement
VS1	"I saw the virtual environment get smaller or larger"
VS2	"I saw the virtual environment flicker"
VS3	"I saw the virtual environment get brighter or dimmer"
VS4	"I saw that something in the virtual environment had changed color"
VS5	"I felt like my field of view was changing in size"
VS6	"I felt like I was getting bigger or smaller"
VS7	"I saw that something in the virtual environment had changed size"

A APPENDIX

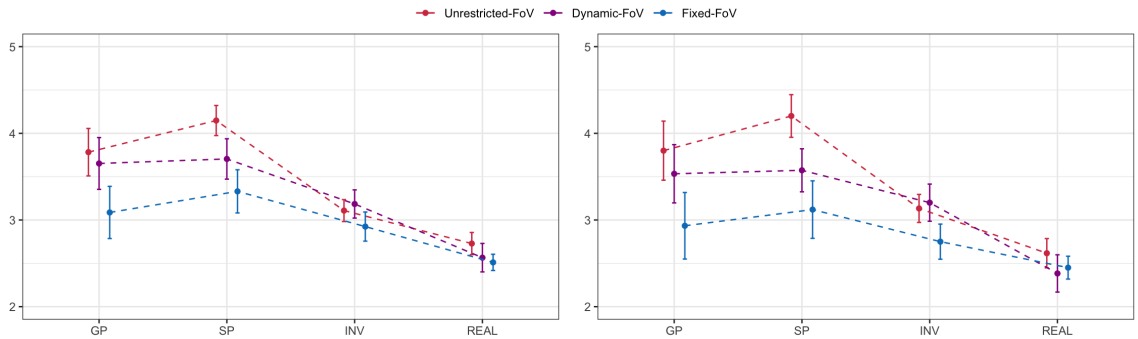

Fig. 5. Mean scores and standard errors for the full population (left) and upper 75th percentile subpopulation (right)

Table 5. Mean scores and standard errors for SSQ and VRSQ components across conditions *unrestricted-FoV*(u-FoV), *dynamic-FoV*(d-FoV), and *fixed-FoV*(f-FoV), considering the full population (top) and upper 75th percentile subpopulation (bottom). Total Severity (TS) scores are highlighted in light grey

			Unrestricted-FoV	*Dynamic-FoV*	*Fixed-FoV*
Full	SSQ	TS	16.75 ± 3.21	9.76 ± 4.24	9.76 ± 2.18
		D	26.63 ± 5.93	15.13 ± 6.77	11.5 ± 3.46
		O	10.22 ± 2.72	5.93 ± 2.94	7.25 ± 2.21
		N	11.61 ± 2.40	7.05 ± 3.51	7.88 ± 2.73
	VRSQ	TS	9.38 ± 1.97	4.53 ± 1.94	3.95 ± 1.17
		D	10.44 ± 2.09	4.35 ± 1.81	3.19 ± 1.25
		O	8.33 ± 2.28	4.71 ± 2.21	4.71 ± 1.56
Upper 75th	SSQ	TS	21.19 ± 4.39	13.21 ± 6.28	9.48 ± 2.8
		D	33.41 ± 8.01	18.56 ± 10.04	12.06 ± 4.87
		O	14.65 ± 3.35	9.60 ± 4.016	8.09 ± 2.61
		N	12.72 ± 3.18	8.90 ± 5.22	5.72 ± 3.20
	VRSQ	TS	12.28 ± 2.56	6.22 ± 2.72	4.28 ± 1.49
		D	12.89 ± 2.56	5.78 ± 2.59	3.56 ± 1.71
		O	11.67 ± 2.79	6.67 ± 3.07	5 ± 1.78

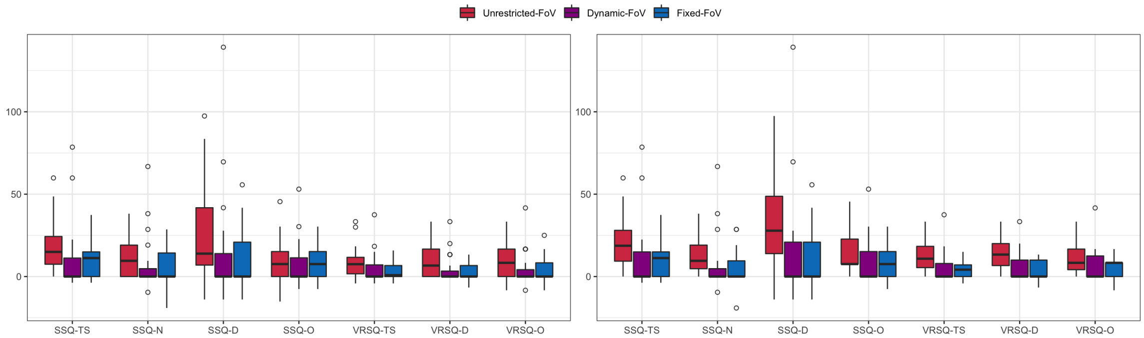

Fig. 6. Boxplots for SSQ and VRSQ components for the full population (left) and upper 75th percentile subpopulation (right)